J. Electroanal Chem., 145 (1983) 225–264
Elsevier Sequoia S.A , Lausanne – Printed in The Netherlands

Review

THE ELECTROCHEMICAL DOUBLE LAYER ON sp METAL SINGLE CRYSTALS

THE CURRENT STATUS OF DATA

A. HAMELIN

Laboratoire d'Electrochimie Interfaciale du C.N.R.S., 1, Place Aristide Briand, 92195 Meudon-Bellevue (France)

T. VITANOV

Central Laboratory of Electrochemical Power Sources of B.A.S., Sofia 1040 (Bulgaria)

E. SEVASTYANOV

Institute of Electrochemistry of the Academy of Sciences of the U.S.S.R., 117071, Moscow V-71, Leninsky Prospekt, 31 (U.S.S.R.)

A. POPOV

Central Laboratory of Electrochemical Power Sources of B.A.S., Sofia 1040 (Bulgaria)

(Received 1st July 1982, in revised form 26th August 1982)

ABSTRACT

This complete review of double-layer data obtained with single-crystal faces of sp metals includes seven tables summarizing all data obtained to date and 158 references. Comparison of these data is made, and comparison with data obtained with polycrystalline electrodes is discussed

(I) INTRODUCTION

The basic concepts of the structure of an electrode–electrolyte interface were developed from experimental data at the mercury–aqueous solution interface. Experimental results obtained for liquid amalgams and another pure metal, gallium, have raised a question: How does the nature of the metal influence the properties of the electrode–electrolyte interface? To answer this question, a large number of solid metals were investigated and a considerable amount of experimental data was accumulated.

It was suggested that some of the difficulties encountered in quantitative interpretation of the double-layer (dl) capacitance measurements for solid electrodes were connected with the crystallographic non-uniformity of their surfaces [1]. Then a large number of experimental results were obtained with solid single-crystal electrodes. It is high time that attempts are made to draw conclusions about the general influence

0022-0728/83/0000–0000/$12.00

of the crystallographic orientation (co) on the dl structure and behaviour. Here we review data on sp metal single faces, numerous for some metals and scarce for others.

In discussing the electrochemical dl at metal single-crystal electrodes in contact with an electrolytic solution, one has to go back as far as 1956–57 when potentials of zero charge (pzc) for low-index faces of zinc were published [2,3]. They were obtained from the minimum of the differential capacity vs. potential curves [$C(E)$] in dilute solution. However, the importance of the physical state of the surface on the dl for solid electrodes had already been pointed out in 1928 by Frumkin [1]. Owing to the dependence of the electronic work function on the orientation of single-crystal faces [4], a difference in their dl parameters would be expected. One of us [5], reviewing studies on flat single-crystal metal electrodes up to May 1968, gave 11 references concerning dl studies on sp metal faces, namely two on zinc [2,6], two on silver [7,8], six on gold [9–14] and one on copper [15]. From then on the number of papers dealing with this particular subject has increased regularly.

(II) ELECTRODE PREPARATION TECHNIQUES

(II.1) Crystal growth

Electrochemists who wish to grow their own single crystals may refer to universally accepted works [16,17]. Either conventional solid single-crystal faces or films of given crystallographic orientation may be used.

Conventional single crystals, according to the metal and the laboratory facilities, are grown from the melt either in a crucible (graphite for silver and gold [11], quartz, etc.) or by zone melting.

Metal film electrodes of preferential crystallographic orientation were prepared, for instance on cleaved mica for the (111) face of gold [18] and on sodium chloride crystals for the (100) face of gold [19]. However, in the case of sputtered gold on mica grain boundaries exist at the surface and could interfere with the electrochemical results. Sputtered silver on conventional silver electrode has been shown to oxidize in air; this oxide cannot be reduced electrochemically [20]. It can be understood that sputtering in vacuum cannot be used for surface preparation for all metals.

(II.2) Preparation and isolation of the electrode surface

(II.2.1) Cutting and polishing

For hexagonal close-packed metals it is possible to cleave the crystals along the most densely packed face [6], thus cutting and polishing are avoided.

For most conventional solid single crystals cutting is necessary. When electrolytic growth is foreseen, the crystal is etched and faces of low indices appear; the crystal is then shaped such that the desired face is perpendicular to the axis of the crystal. Other conventional single crystals are either ground or cut (with a thread saw or by

spark erosion) along the desired orientation. The removal of the disturbed layer which exists at the surface after cutting is generally done by first making this layer thinner by mechanical polishing (with emery paper, then alumina or diamond pastes of different grades), and in some cases electrochemical polishing is necessary. This is the most tedious part of surface preparation. To achieve it the crystal must be placed in a holder (araldite, Teflon, etc.), and positioning in this holder can entail surface disorientation. This method allows faces of any crystallographic orientation to be obtained and thus the variation of dl parameters can be seen from a general viewpoint.

(II.2.2) Surface preparation

After mechanical polishing, electrochemical or chemical polishing or ion bombardment is sometimes necessary to remove the disturbed layer completely. For each metal a specific technique must be used. The final surface preparation is either annealing at high temperature or sputtering of the same metal (homo-epitaxy) to diminish the surface defects.

Electrochemical crystal growth in a capillary [21–24], used to prepare silver single-crystal electrodes of (100) and (111) orientations, gives excellent results for dl measurements without final surface preparation. A mother crystal grown by the Bridgman method was used to obtain monocrystalline filaments grown in glass or Teflon capillaries so that only one crystallographic face filled the section of the capillary. The surface of the face consisted of smooth terraces and growth steps; by convenient cathodic treatment one can change the growth-step density and can thus partly modify the atomic surface structure of the electrode, although its co remains unchanged [25]. In fact the possibility to change, at will, this density is the main advantage of this type of electrode; this is impossible for the other electrodes mentioned here. Electrodes either without growth steps or with minimal growth-step densities were thus obtained. It should be emphasized that in this way the possible existence of atomic irregularities of the surface structure is limited. Furthermore, the influence of these atomic irregularities on dl measurements was studied by using faces with a definite growth-step density (from 2 to 20×10^4 cm^{-1}).

(II.2.3) Isolation of the face of interest

The faces grown in a capillary do not need further isolation. This is not the case for other types. Very often, just embedding in Teflon is used. But to avoid creeping of the electrolyte between the crystal and its holder, isolation is often ensured by RTV silicone or by polythene dissolved in toluene; in any case it should be a non-contaminating material. When using films special holders are used (with an O-ring) which can also be used for crystals of large geometric area for optical measurements.

(II.3) Checking of the physical and chemical states of electrode surfaces

The state of the electrode surface is first checked by ex situ methods for the co, the definite physical state and the chemical cleanness of the surface. These points will be examined.

After surface preparation, most single-crystal electrodes are checked by an X-ray back-diffraction Laue method to confirm the co of the surface. Generally, it is known within an error of about $\pm 2°$. Only recently the co was checked by a self-collimation technique, and then it was known within $\pm 0.3°$ [26]. But X-rays penetrate more than 1000 atomic layers into the metal, and so they give no information about the top layer of atoms at the surface where electrochemistry is performed. Obviously, cleaved surfaces and electrolytically grown crystals do not need this checking of the average co. In the latter case, checking of the co was done by observing the shape of the growing face [24,25].

Orientation of film electrodes was checked by electron diffraction [18].

A number of electrochemists now check their surfaces with LEED, and it can be understood that all methods developed recently in surface physics may be applied to single-crystal electrodes.

Besides the co, the surface must have as few defects as possible because dl properties are observed on all the surface in contact with solution. For checks, conventional methods were used: optical microscopy, electron microscopy, etc. These ex situ methods deal with the physical state of the surface. The chemical state should be checked by Auger spectroscopy.

In the case of crystals grown electrolytically in capillaries, the exchange current density in $AgNO_3$ which is very sensitive to growth-step density is used to check the state of the surface before and after dl measurements [25,27].

For all ex situ checking there is the problem of transfer to and from the electrochemical cell where dl measurements are performed. Therefore in situ checks are absolutely necessary. Most of the in situ checks are provided by direct current–potential curves $i(E)$ and differential capacity–potential curves $C(E)$, i.e. by the electrochemical results themselves:

(1) The $i(E)$ curves because they are very sensitive: to the creeping of solution between the crystal and the isolating material, to chemical contamination of the surface and in some cases (gold, for instance)—in the oxide formation and reduction regions—to the physical state such as the co.

(2) $C(E)$ curves also provide a check of the surface state in the following ways: frequency dispersion allows the range of potential in which the electrode is ideally polarizable to be determined, it also allows creeping of solution to be detected and it is sensitive to the roughness of the electrodes; the shape and the position of the minimum corresponding to diffuse-layer behaviour give indications of the cleanliness of the physical state and quality of the surface. Optical methods (ellipsometry, electroreflectance, etc.) are being used more and more in dl studies of sp metals: it was shown that the symmetry properties of the crystalline faces were not perturbed by contact with aqueous solutions [28–30]. Last but not least, the reproducibility of the electrochemical results confirms the quality of the surface of the electrode.

Nevertheless, with single-crystal electrodes some problems remain.

(1) The effect of the edge; the smaller the crystal the more important is the effect. In whatever way the junction is made with the insulating material which prevents the contact of other crystallographic orientations with the electrolytic solution, this is

never "perfect" (crystal grown in capillaries, O-ring positioned on the crystal surface, isolation of the face of interest by RTV silicone).

(2) The precision of the co, which was discussed above; in most of the references in this paper precision of the co is not given.

(3) All possible defects may exist at the metal surface: on an atomic scale (dislocations [31], vacancies, twinning, polygonization, etc.) and larger irregularities in the atomic arrangement due to scratches, pits (from electrochemical polishing for instance).

They all in fact change the surface and they entail crystallographic anisotropy which makes quantitative analysis difficult. Most of these defects are avoided on electrolytically grown faces.

(III) EXPERIMENTAL RESULTS

Most experimental results on sp metals were obtained with silver and gold, which crystallize in the same face-centered cubic systems (fcc). In this system the (111) face is the most close packed, and has a symmetry of the third order; it is often called the octahedral face. The (100) face or cubic face is less close packed and has a symmetry of the fourth order. The (110) face is made of compact "rails" of atoms along the ⟨110⟩ axis with hollows in between, and is corrugated on an atomic scale. These

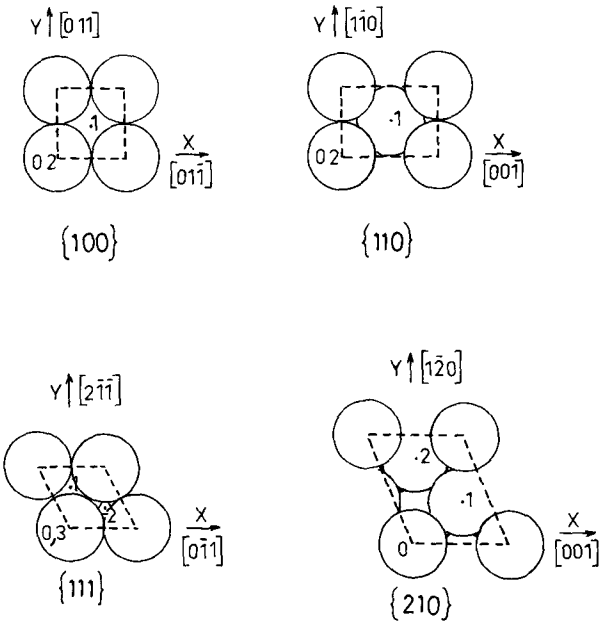

Fig. 1 Atomic positions of the (100), (110), (111) and (210) faces in the fcc structure, 0, 1, 2, 3 are layers of atoms, 0 being the outermost layer The shapes and dimensions of the primitive unit cells are shown (— — —) [32].

three faces for the fcc system are shown in Fig. 1. The (210) face is also given for comparison.

Not only were faces of simple Miller indices studied but also higher Miller index faces which can be tentatively described by the TLK (terraces, ledges, kinks) model; descriptive notations are available [33].

Some experimental results on metals other than silver and gold, e.g. lead and copper which are fcc and zinc which is hexagonal close packed (hcp), were published. Data on bismuth regarded as a semi-metal and which is rhombohedral will be given.

All figures were redrawn following the IUPAC recommendations. All potentials are given vs. SCE. No dissertation work is given in the references.

(III.1) Silver

Silver belongs to the first group of the periodic table, its electronic structure is $5s^1$. It crystallizes in the fcc system, its melting-point is 960.8°C. For crystal growth see section (II.2).

A general survey of the published results concerning dl on silver faces is given in Table 1.

The earliest study on dl of separate faces of silver deals with the effect of dislocations and surface imperfections on the dl capacity [7]. The first $C(E)$ curves

TABLE 1

Data obtained on silver faces

Co in Miller indices	Solutions	E_{min} in the most dilute solution or pzc vs. SCE/V	Adsorption	Ref	Year
(111)	200 mM H_2SO_4			7	1965
(111)	5 mM Na_2SO_4			8	1967
(111)	2.5–10 mM Na_2SO_4	-0.74 ± 0.02	No	34	1969
(111)	2.5–25 mM K_2SO_4	-0.75	Yes	50	1969
(111)	5–40 mM NaF	$-0.69 + 0.01$ [a]	No	35	1971
(111)	5 mM Na_2SO_4	$-0.72 + 0.02$	No	36	1972
(111)	1–10 mM KF	-0.70 ± 0.02 [a]	No	36	1972
(111)	5–40 mM NaF	-0.69 ± 0.01 [a]	No	37	1973
(111)	0.5–25 mM Na_2SO_4	-0.76 ± 0.01	No	52	1974
(111)	5–100 mM K_2SO_4		Yes	51	1974
(111)	50 mM Na_2SO_4 + n-hexanol		Yes	59	1974
(111)	2.5–50 mM Na_2SO_4	-0.76 ± 0.01	No	25	1975
(111)	2.5–5 mM Li_2SO_4	-0.76 ± 0.01	No	158	1975
(111)	2.5–5 mM Cs_2SO_4	-0.74 ± 0.01	Yes	158	1975
(111)	1–50 mM $NaNO_3$	-0.74 ± 0.01	No	25	1975
(111)	50 mM Na_2SO_4 + isobutanol		Yes	56	1976

TABLE 1 (continued)

Co in Miller indices	Solutions	E_{min} in the most dilute solution or pzc vs SCE/V	Adsorption	Ref	Year
(111)	5 m*M* Na_2SO_4	−0.76±0 01	No	54	1977
(111)	(100− *x*)m*M* KF+ *x* m*M* KCl (*x* = 1–40)	−0.76±0 01	Yes	54	1977
(111)	(100− *x*)m*M* KF+ *x* m*M* KCl, KBr (*x* = 1–40)		Yes	55	1978
(111)	5 m*M* Na_2SO_4	−0.76±0 01	Yes	55	1978
(111)	10–40 m*M* KCl, KBr, KI		Yes	49	1978
(111)	NaF		No	47	1978
(111)	(40− *x*)m*M* NaF+ *x* m*M* NaCl (*x* = 0.2–40)		Yes	49	1978
(111)	500 m*M* $NaClO_4$			62	1980
(111)	500 m*M* $NaClO_4$			63	1980
(111)	100 m*M* NaCl+pyridine			63	1980
(111)	10 m*M* NaF+S			20	1981
(111)	100 m*M* NaF+ *x* m*M* NaCl (*x* = 0 1–300)		Yes	60	1981
(111)	100 m*M* NaF+pyridine		Yes	60	1981
(111)	20 m*M* NaF+diethylether		Yes	104	1982
(111)	2–100 m*M* KF	−0.700±0 002 [a]	No	39	1982
(111)	2–100 m*M* $NaClO_4$	−0.720±0 003	Yes	39	1982
(111)	5 m*M* Na_2SO_4		Yes	27	1983
(111)	500 m*M* NaF			64	1983
(100)	2,5–10 m*M* Na_2SO_4	−0 89±0 02	No	34	1969
(100)	2.5–25 m*M* K_2SO_4	−0.84	Yes	50	1969
(100)	5–40 m*M* NaF	−0 91±0 01 [a]	No	37	1973
(100)	0.5–50 m*M* Na_2SO_4	−0.91±0.01	No	52	1974
(100)	5–100 m*M* K_2SO_4		Yes	51	1974
(100)	50 m*M* Na_2SO_4 + *n*-hexanol		Yes	59	1974
(100)	2.5–25 m*M* Na_2SO_4	−0.91±0.01	Yes	25	1975
(100) [b]	5 m*M* Na_2SO_4	−0.85±0 01 [a,c]	No	25	1975
(100)	2.5–5 m*M* Li_2SO_4	−0.91±0.01	No	158	1975
(100)	2 5–5 m*M* Cs_2SO_4	−0 89±0 01	Yes	158	1975
(100)	50 m*M* Na_2SO_4 + *n*-amyl alcohol		Yes	25	1975
(100)	2–100 m*M* KF	−0 85±0.01 [a]	No	25	1975
(100)	1–10 m*M* $NaNO_3$	−0.90±0.01	Yes	25	1975
(100) [b]	5 m*M* Na_2SO_4	−0.85±0.01 [a,c]	No	53	1976
(100)	2–100 m*M* KF	−0 85±0.01 [a]	No	38	1976
(100)	2–10 m*M* KCl, KBr, KI		Yes	38	1976
(100)	50 m*M* +isobutanol		Yes	56	1976
(100)	(100− *x*)m*M* KF+ *x* m*M* KCl (*x* = 1–40)		Yes	54	1977
(100)	(100− *x*)m*M* KF+ *x* m*M* KBr (*x* = 1–40)		Yes	55	1978
(100)	NaF		No	47	1978
(100)	10–40 m*M* KCl, KBr, KI		Yes	49	1978

(continued on p 232)

TABLE 1 (continued)

Co in Miller indices	Solutions	E_{min} in the most dilute solution or pzc vs SCE/V	Adsorption	Ref	Year
(100)	$(40+x)$mM NaF $-x$ mM NaCl ($x = 0.2$–40)		Yes	49	1978
(100)	500 mM $NaClO_4$			63	1980
(100)	10 mM NaF + S		Yes	20	1981
(100)	100 mM NaF + x mM NaCl ($x = 0.1$–300)		Yes	60	1981
(100)	100 mM NaF + pyridine		Yes	60	1981
(100)	20 mM NaF + diethylether		Yes	104	1982
(100)	5–100 mM $NaClO_4$, NaF		Yes	48	1982
(100)	5–100 mM KPF_6	-0.865 ± 0.003 [a]	No	48	1982
(100)	$(20-x)$mM KPF_6 + x mM NaF, $NaClO_4$ ($x = 1.25$–20)		Yes	48	1982
(100)	500 mM NaF			64	1983
(100)	2–100 mM KF	-0.850 ± 0.002 [a]	No	39	1982
(100)	2–100 mM $NaClO_4$	-0.894 ± 0.003	Yes	39	1982
(110)	200 mM H_2SO_4			7	1965
(110)	2.5–25 mM K_2SO_4	-0.90	Yes	50	1969
(110)	5–40 mM NaF	-1.01 ± 0.01 [a]	No	45	1971
(110)	5–40 mM NaF	-1.01 ± 0.01 [a]	No	37	1973
(110)	5 mM Na_2SO_4	-0.96 ± 0.01		52	1974
(110)	5–100 mM K_2SO_4		Yes	51	1974
(110)	NaF		No	47	1978
(110)	10–40 mM KCl, KBr, KI		Yes	49	1978
(110)	$(40-x)$mM NaF + x mM NaCl ($x = 0.2$–40)		Yes	49	1978
(110)	500 mM $NaClO_4$			62	1980
(110)	500 mM $NaClO_4$			63	1980
(110)	10 mM NaF + S		Yes	20	1981
(110)	100 mM NaF + x mM NaCl ($x = 0.1$–300)		Yes	60	1981
(110)	5–100 mM $NaClO_4$, KPF_6, KBF_4	-0.975 ± 0.005 [a]		40	1981
(110)	100 mM NaF + pyridine		Yes	60	1981
(110)	$(40-x)$mM NaF + x mM NaBr ($x = 0.125$–40)		Yes	57	1982
(110)	20 mM NaF + diethylether		Yes	104	1982
(110)	500 mM NaF			64	1983
(210)	10 mM NaF		No	49	1978
(210)	10 mM KCl, KBr, KI		Yes	49	1978
(211)	200 mM H_2SO_4			7	1965

[a] E_{min} is said to coincide with the pzc.
[b] The face is said to be dislocation free.
[c] After correction for electrolyte asymmetry

of separate faces of silver were obtained in dilute solutions of Na_2SO_4 [8,34]. The electrodes were prepared by electrolytically growing silver single crystals in glass capillaries. Later the measurements were carried out in dilute solutions of NaF, KF and Na_2SO_4 on electropolished electrodes, embedded in Teflon holders [35–37], as well as on electrodes electrolytically grown in Teflon capillaries [25,38,39]. In all cases the preliminary surface preparation included electroreduction of the surface by a cathodic current. At the minimum of the $C(E)$ curves the frequency dispersion was $< 10\%$ from 210 to 2000 Hz and the residual current $< 10\ \mu A\ cm^{-2}$ for electrolytically grown faces and 5% from 20 to 320 Hz for electropolished faces [40].

The most reliable data for *the pzc* determined from E_{min} of the $C(E)$ curves in aqueous KF, NaF and KPF_6 solutions which were said to be not specifically adsorbed, have the values vs. SCE of -0.700 ± 0.002 V for (111) [39], -0.850 ± 0.002 V for (100) [39] and -0.975 ± 0.005 V for (110) [40]. The pzc of the polycrystalline silver was found to be close to that of the (110) face, -0.94 to -0.98 V [37,41,42]. It is clear that the pzc is markedly dependent on the co. This dependence, first predicted in ref. 1, is in qualitative accordance with the known relation between the pzc and the electronic work function [43], together with the known dependence of the work function on the crystal face [4,44].

The validity of the dl theory in the absence of specific adsorption for different faces of silver has been proved [25,35,37–39,45]. At E_{min} a linear dependence of C^{-1} vs. C_d^{-1} (Parsons–Zobel plot) in 2–100 mM KF has been obtained [25,38,39]. The reciprocal slope is close to unity (1.02–1.04) and does not depend on the co, while in ref. 37 it is larger and increases with the atomic roughness of the face ($f_{(111)} = 1.10$,

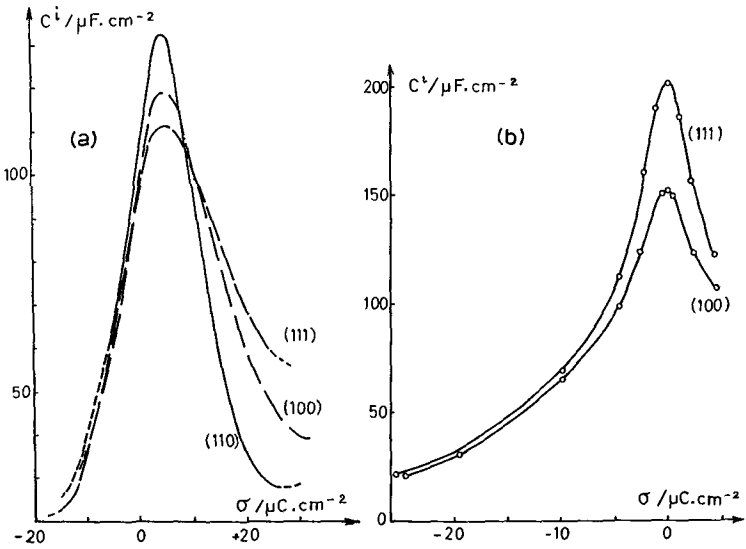

Fig 2. $C'(\sigma)$ curves: (a) for electropolished (100), (110) and (111) faces of silver in aqueous NaF [37]; (b) for electrolytically grown (111) and (100) faces of silver in aqueous KF [39]

$f_{(100)} = 1.15$, $f_{(110)} = 1.20$). These facts were also observed for polycrystalline silver [41].

The *inner-layer capacity–charge curve* [$C^1(\sigma)$] for low-index faces has been calculated [35,37] (Fig. 2a). It has a high maximum and is almost independent of the co at $\sigma = 0$ while showing a more marked dependence at positive charges. The origin of the maximum is still not quite clear. The most probable explanation according to ref. 37 is that of the reorientation of water molecules adjacent to the metal surface. Other authors (Fig. 2b) observed a clearly expressed dependence of C^1 on co at $\sigma = +5\ \mu C\ cm^{-2}$ up to moderate negative charges. Besides the larger values of C^1 for (111) and (100) faces, at $\sigma = 0$, than that in ref. 37, the dependence of C^1 on co was explained [39] to be due to the different hydrophilicity of the faces and/or the different structure of the water layer on the metal surface. The discrepancy in the slope of the Parsons–Zobel plots, as well as the inner-layer capacity calculated in refs. 37 and 38, is said to be connected to the influence of defects of the electrodes, used in ref. 37, on C at E_{min} [46], but the higher value of the reciprocal slope of the (110) face has been shown [40] to be due to a weak specific adsorption of F^- on this face.

The structure of the inner part of the dl was discussed for water [47] and ions [39,40,48], and in some cases the components of C^1 were calculated [40,48,49].

The first papers on *adsorption of inorganic ions* on single-crystal surfaces of silver are those on SO_4^{2-} [50,51]. A clearly expressed concentration dependence of E_{min} on electropolished (111), (100) and (110) faces in dilute solutions of K_2SO_4 was observed. On the other hand, other data [25,34,52,158] have shown that in similar conditions no concentration dependence of E_{min} on electrolytically grown faces, as well as on electropolished (111) and (100) faces, exists. The contradiction was elucidated [25,53–55] by studying the effect of the preparation conditions of the

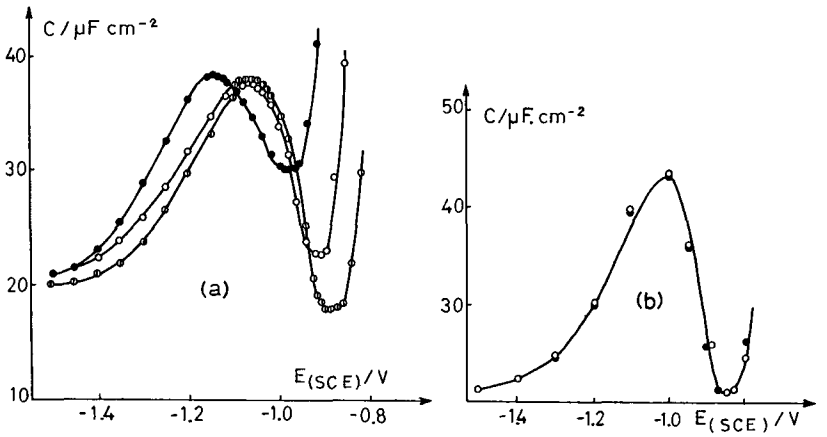

Fig. 3 $C(E)$ curves of an electrolytically grown (100) face of silver for different step densities L: (a) in 5 mM Na_2SO_4, $L = 0$ (Φ); 2×10^4 (○), 14×10^4 cm^{-1} (●); (b) in 10 mM KF, $L = 1.9\times10^4$ (○); 13.5×10^4 cm^{-1} (●) [25].

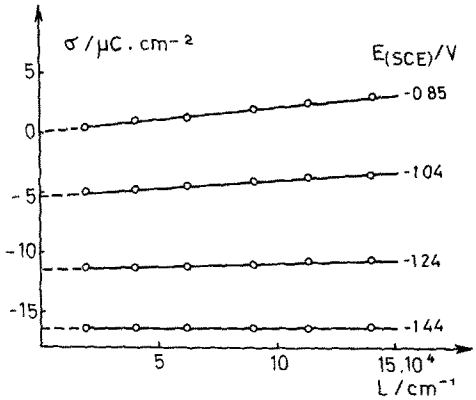

Fig 4. The $\sigma(L)$ dependence at different E for an electrolytically grown (100) face of silver in 5 mM Na_2SO_4 [27,54,55]

surface on the dl capacity of the (111) and (100) faces. It was shown that at a constant concentration of dilute solution of Na_2SO_4 the shape of the $C(E)$ curve depends markedly on the length of the growth steps on the surface, while in a solution of KF it does not (Fig. 3a, b). This was explained to be due to the specific

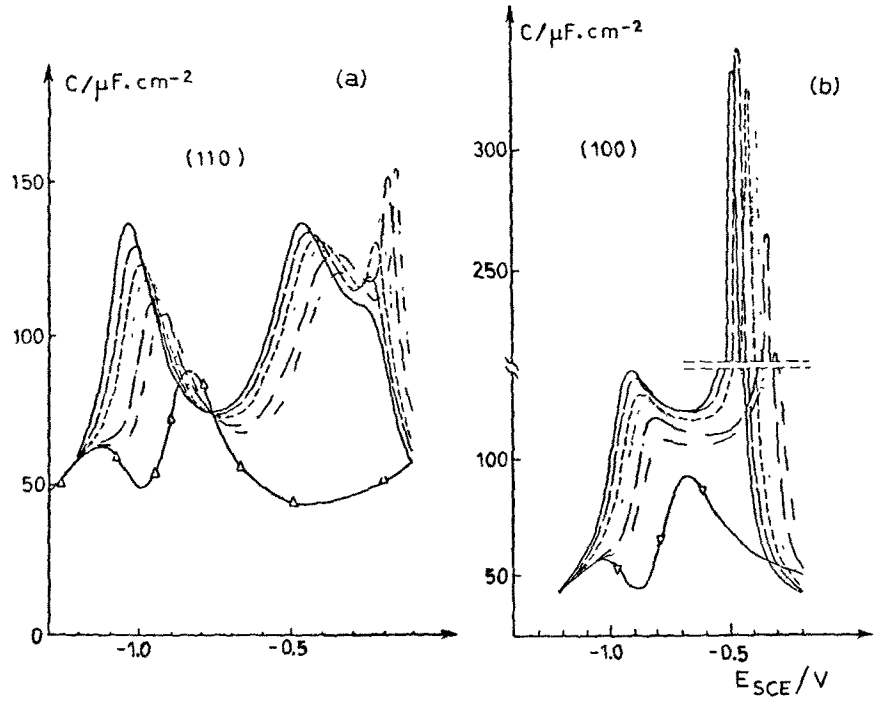

Fig. 5. $C(E)$ curves for electropolished (110) and (100) faces of silver in x mM NaCl + (40 − x)mM NaF from $x = 0$ (–△–) to $x = 40$ (———) [49].

adsorption of SO_4^{2-} on the steps only. The charge of SO_4^{2-}, adsorbed on the steps, was estimated quantitatively [27,54,55]. A linear relation between total charge of the surface, σ, and step density, L, has been found (Fig. 4), which was interpreted as proving that the total charge is a sum of the charge of terraces and that of the steps. Then the charge of the ions specifically adsorbed per unit step length and that of the terraces were estimated from the slope and from the intercept of the plot σ/L.

The adsorption of halide ions on the single-crystal surface of silver has been studied the most thoroughly so far [25,38,49,54,55,57]. The shape of the $C(E)$ curves in aqueous KCl, KBr and KI is typical for the case of strong specific adsorption. A markedly expressed minimum reflecting the contribution of the diffuse dl was observed only in 2 mM KCl for the (100) face [25,38]. In many cases three peaks on $C(E)$ curves may be seen, as for example with the adsorption of Cl^- on the (110) face (Fig. 5a) [49]. A detailed thermodynamic analysis of the adsorption of Cl^- on a (110) face from mixed solutions of NaCl + NaF at constant ionic strength has shown that the most negative peak occurs at quite low coverage ($< 10\%$) and is said to be due to the reorientation of water molecules in the inner layer. The middle peak occurs in the range of half coverage and has been interpreted as being caused by the usual type of adsorption effect. The third very narrow peak appears at a more positive potential where the chloride coverage is almost complete. Several explanations for the origin of this peak are given in ref. 49, but the most likely seems to be that related to a partial charge transfer occurring over a narrow potential range. A similar analysis of the adsorption of Br^- on a (110) face from mixed solutions of NaBr + NaF has been carried out in [57]. Clear evidence for a competitive adsorption of F^- within the most negative peak was established when the Br^- concentration is small with respect to the F^- concentration.

The strength of halide adsorption at a given charge on all the faces investigated and the polycrystalline silver [58] increase in the sequence $Cl^- < Br^- < I^-$, while on different faces the sequence is (111) > (100) > (110). This was proved by comparing the C at the same rational potentials [38,54,55], the pzc in the presence and in the

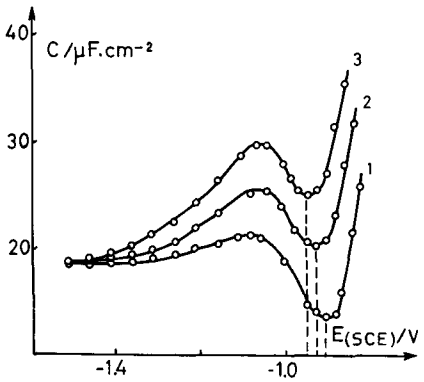

Fig. 6. $C(E)$ curves of an electropolished (100) face of silver in (1) 1, (2) 5 and (3) 10 mM $NaNO_3$ [25].

absence of specific adsorption [49], the Esin and Markov coefficients and the charge due to specifically adsorbed ions at a given σ [27,54,55].

No influence of the step density L on the shape of the $C(E)$ curves in halide-containing solutions has been observed [27,55]. This was explained as being due to the negligible contribution of the charge on the steps which is obscured by the strong adsorption on the terraces.

A markedly expressed concentration dependence of E_{min} for the (100) face [25] (and for the polycrystalline silver [58]) has been observed in solution of $NaNO_3$ (Fig. 6).

Studies on the dl properties of silver faces in dilute solutions of ions which exert a "structure-breaking" effect on water, e.g. ClO_4^-, PF_6^-, BF_4^-, are still in progress. A slight concentration-dependent shift of E_{min} has been observed on the (110) and (100) faces in NaF, $NaClO_4$, KPF_6 and KBF_4 solutions [40,48]; the conclusion was that the strength of the specific adsorption follows the sequence $F^- > ClO_4^- > PF_6^- = BF_4^- \geqslant 0$, for the (110) face, while for (100) the order is $ClO_4 > F^- > PF_6 \geqslant 0$ [48]. Some peculiarities have been observed in the $C(E)$ curves of the (111) and (100) faces in $NaClO_4$ compared to those in KF solutions [39]: (1) a small concentration-independent shift of E_{min} to more negative potentials; (2) higher values of the reciprocal slope of C^{-1} vs. C_d^{-1} plots for the (111) face and a non-linear relationship for the (100) face. These peculiarities were interpreted to be due to a weak specific adsorption of ClO_4^- which is stronger on the (100) face. The data obtained are interpreted by competition between the "squeezing-out" effect of water and the different structure or chemisorption energy of water on these faces. A slight adsorption of F^- compared to ClO_4^- was also observed on polycrystalline silver [39]. The adsorption behaviour of both the (110) face and polycrystalline silver is ascribed to the defects of the electrode used [39].

A few papers have been published on the *adsorption of organic substances* on silver surfaces: *n*-hexyl, isobutyl, *n*-amyl alcohol, pyridine and diethylether (see Table 1). The adsorption of these substances was studied by $C(E)$ curves. At a given frequency of the ac signal the curves exhibit sharp adsorption–desorption peaks, the potential of which at a given concentration depends on the co and on the nature of the organic substance adsorbed. The adsorption of alcohols on the (111) and (100) faces follows a Frumkin isotherm. No dependence of the adsorption energy in terms of the logarithm of the equilibrium constant on the co has been found, i.e. the position of the adsorption–desorption peaks is due to the different pzc alone. On the other hand, the adsorption of *n*-amyl alcohol on polycrystalline silver has been shown to obey a Temkin isotherm [61]. The difference in the type of isotherm on single crystals and polycrystalline electrodes was interpreted as a result of the more regular atomic structure of the former [56,59].

The influence of the growth-step density, L, on the adsorption of *n*-amyl alcohol has been studied [25]. It was shown that at a constant concentration the shape of the $C(E)$ curves depends markedly on the step density and on the base electrolyte. In a solution of KF the $C(E)$ curves are independent of L (Fig. 7a), while in Na_2SO_4 solution some peculiarities may be seen (Fig. 7b): with the increase of L the

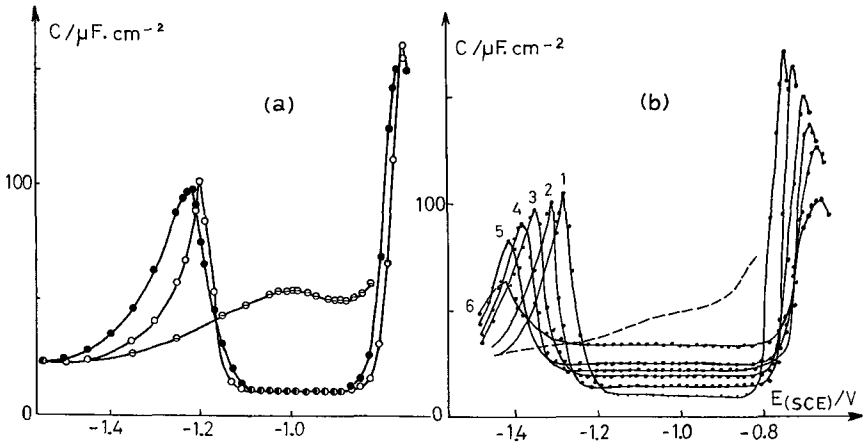

Fig. 7. $C(E)$ curves of an electrolytically grown (100) face of silver with different step densities L: (a) in 100 mM KF + 100 mM $nC_5H_{11}OH$, $L = 1.9 \times 10^4$ (○), 14.1×10^4 cm^{-1} (●); in pure 100 mM KF (⊖), (b) in 50 mM Na_2SO_4 + 300 mM $nC_5H_{11}OH$, $L = 1.5 \times 10^4$ (1); 2.7×10^4 (2), 5.9×10^4 (3), 8.1×10^4 (4), 19.8×10^4 (5), 30×10^4 cm^{-1} (6), in pure 50 mM Na_2SO_4, $L = 1.9 \times 10^4$ cm^{-1} [25]

capacitance in the range of maximum adsorption increases and the adsorption range widens. These peculiarities of the $C(E)$ curves are explained by the competition between SO_4^{2-} occupying the steps, and the adsorbing organic molecules. A similar competitive adsorption of ions and organic molecules has been observed in the case of adsorption of pyridine in the presence of Cl^-. Thus, the adsorption of pyridine is strong on the (110) face and weaker on the (111) and (100) faces because Cl^- ions are more strongly adsorbed on these faces [60].

Some *optical measurements* were performed on silver faces. For the (110) face the electroreflectance spectra at normal incidence differs markedly when the electric field vector of the light is parallel or perpendicular to the surface atomic rails [28]. This reflects the anisotropy in the surface optical constants. Understanding of the interface electronic properties for the (110) and (111) faces was improved by studying surface plasmon excitation (in the case of attenuated total reflection); the dielectric function varies with co and, for the (110) face, with the crystallographic direction [62]. By this last method it was shown that a surface complex between silver (111) and pyridine exists [63] in the dl region.

Surface states (strongly localized at the surface) depend on the electric field of the dl; study of this effect can be used as a probe for the metal–electrolyte interface, and this was done by electroreflectance measurements for the three faces of simplest indices of silver and gave information about the microscopic structure of the inner part of the dl [64].

(III.2) Gold

In the periodic classification of the elements gold is the last of the sp metals, close to the d-metals. Its electronic structure is $(5d^{10})\ 6s^1$, its electronic d-band is

complete. Its melting-point is 1063°C. Gold crystallizes in the fcc system. For crystal growth and electrode preparation, see section (II).

It was observed with polycrystalline gold that in a range of potential of about 1 V there is no faradaic reaction [65,66]; so gold seemed suitable for studying the influence of the co of the surface of the electrode on the dl parameters.

Some of the earliest work on the dl at single-crystal–aqueous solutions was done with gold [9,10].

For gold, the *verification of the cleanness* of the electrochemical interface is conveniently done by recording a cyclic voltammogram (CV): a triangular potential excursion is imposed on the gold face with instantaneous recording of the current. The CV obtained is of the type shown in Fig. 8 [67] for the (210) face in 10 m*M* NaF. Three types of processes are responsible for the current:

(1) change of the electrostatic charge on the metal (and in solution) in the dl region; we are interested in this process in this review paper;

(2) pseudo-capacitive charging current with charge transfer for the formation of a monolayer of oxygen on the gold face (or reduction of this monolayer) (this process is used to check the cleanness of the interface and the shapes of the peaks are characteristic of the co);

(3) faradaic current, in this case reduction of the solvent.

When there is strong specific adsorption of the anion, process (2) cannot be

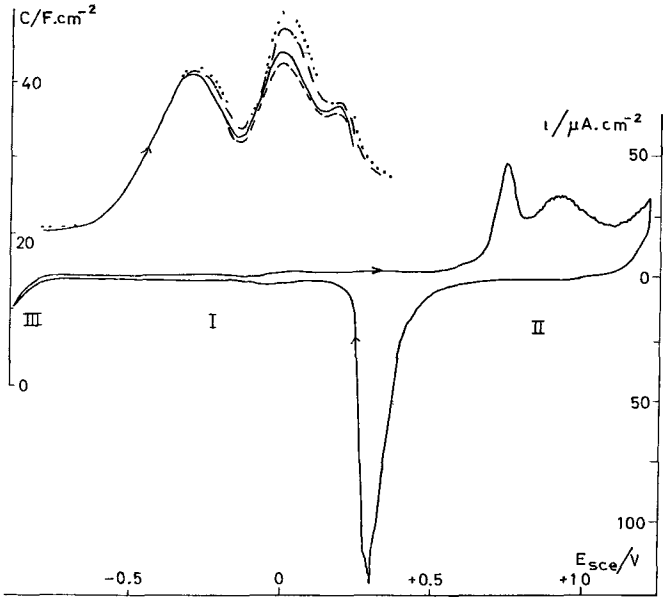

Fig 8. Cyclic voltammogram of a (210) face of gold, 10 m*M* NaF, sweep rate 20 mV s^{-1} $C(E)$ curves for a (210) gold face in 40 m*M* NaF (· · ··) 15 Hz, (-·- -) 20 Hz; (———) 40 Hz; (— — —) 80 Hz, sweep rate 10 mV s^{-1} [67]

TABLE 2

Data obtained on gold faces

Co in Miller indices	Solutions	E_{min} in the most dilute solution or pzc, vs SCE/V	Adsorption	Ref	Year
(111)	200 mM K_2SO_4		Yes	11	1967
(111)	12.5–200 mM K_2SO_4		Yes	12	1968
(111)	200 mM K_2SO_4 + pyridine		Yes	13	1968
(111)	2.5–10 mM K_2SO_4		Yes	68	1969
(111)	2.5–20 mM NaF	+0.26±20	No	69	1971
(111)	10–20 mM KBr		Yes	70	1971
(111)	5–100 mM KCl		Yes	71	1973
(111)	5–100 mM KI		Yes	72	1973
(111)	5 mM K_2SO_4	+0.12	Yes	73	1974
(111)	2–50 mM NaF	+0.33±0.02 [a]	No	74	1974
(111) [b]	10 mM NaF	+0.33±0.02 [a]	No	18	1975
(111)	100 mM KCl, KBr, KI		Yes	76	1975
(111) [c]	10 mM NaF	+0.33±0.02 [a]	No	77	1975
(111)	10 mM NaF		No	78	1976
(111)	10 mM NaF	+0.33±0.02 [a]	No	79	1976
(111)	100 mM KI		Yes	80	1978
(111)	20 mM NaF		No	81	1978
(111)	20 mM NaF			82	1978
(111)	10 mM NaF			83	1978
(111) [b]	20 mM NaF			84	1979
(111)	20 mM NaF		No	29	1980
(111)	20 mM NaF (pH = 5.2–10.8)			85	1980
(111)	100 mM KI			86	1980
(111)	20 mM NaF		No	87	1980
(111)	20 mM NaF pH = 5	+0.24 [a]	No	90	1980
(111) [c]	500 mM $NaClO_4$			62	1980
(111)	20 mM NaF + 1 M diethylether		Yes	104	1982
(111)	10 mM NaF pH = 5.6	+0.33±0.01 [a]	No	94	1982
(111)	KI, KBr, KCl, NaF, K_2SO_4			96	1983
(111)	20 mM K_2SO_4 + pyridine		Yes	97	1983
(111)	10 mM NaF + diethylether		Yes	98	1983
(100)	1–1000 mM $HClO_4$		No	9	1962
(100)	200 mM K_2SO_4		Yes	11	1967
(100)	12.5–200 mM K_2SO_4		Yes	12	1968
(100)	200 mM K_2SO_4 + pyridine		Yes	14	1968
(100)	2.5–10 mM K_2SO_4		Yes	68	1969
(100)	2.5–20 mM NaF	+0.14±0.02	No	69	1971
(100)	10–20 mM KBr		Yes	70	1971
(100)	5–100 mM KI		Yes	72	1973
(100)	5 mM K_2SO_4, 5–100 mM KCl, 100 mM KI		Yes	73	1974
(100)	10 mM NaF	+0.14±0.02	No	79	1976
(100)	100 mM KI		Yes	80	1978
(100) [c]	10–40 mM NaF	+0.10±0.01 [a]	No	19	1978

TABLE 2 (continued)

Co in Miller indices	Solutions	E_{min} in the most dilute solution or pzc, vs SCE/V	Adsorption	Ref	Year
(100)	20 m*M* NaF		No	81	1978
(100)	20 m*M* NaF		No	82	1978
(100)	10 m*M* NaF		No	83	1978
(100)	20 m*M* NaF		No	29	1980
(100)	100 m*M* KI		Yes	86	1980
(100)	20 m*M* NaF pH = 5	+0.06 [a]	No	90	1980
(100)	10–20 m*M* NaF (+S)		Yes	20	1981
(100)	20 m*M* NaF + 1 *M* diethylether		Yes	104	1982
(100)	10 m*M* NaF pH = 5.6		No	94	1982
(100)	10 m*M* NaF, 10–500 m*M* $LiClO_4$, 10 m*M* $HClO_4$, 10 m*M* $KClO_4$		Slight	99	1982
(100)	KI, KBr, KCl, NaF, K_2SO_4, $HClO_4$			96	1983
(100)	20 m*M* K_2SO_4 + pyridine		Yes	97	1983
(100)	10 m*M* NaF + diethylether		Yes	98	1983
(100)	500 m*M* NaF			64	1983
(110)	1–1000 m*M* $HClO_4$		No	9	1962
(110)	200 m*M* K_2SO_4		Yes	11	1967
(110)	12.5–200 m*M* K_2SO_4		Yes	12	1968
(110)	200 m*M* K_2SO_4 + pyridine		Yes	13	1968
(110)	2.5–10 m*M* K_2SO_4		Yes	68	1969
(110)	2.5–20 m*M* NaF	−0.05 ± 0.01 [a]	No	69	1971
(110)	10–20 m*M* KBr		Yes	70	1971
(110)	5–100 m*M* KCl		Yes	71	1973
(110)	5–100 m*M* KI		Yes	72	1973
(110)	5 m*M* K_2SO_4	−0.14 ± 0.02 [a]	Yes	73	1974
(110)	5–100 m*M* KCl, KBr, KI		Yes	75	1974
(110)	10 m*M* NaF	−0.05 ± 0.01 [a]	No	79	1976
(110)	100 m*M* KI		Yes	80	1978
(110)	20 m*M* NaF		No	81	1978
(110)	20 m*M* NaF		No	82	1978
(110)	10 m*M* NaF			83	1978
(110)	20 m*M* NaF		No	88	1979
(110)	20 m*M* NaF		No	29	1980
(110)	20 m*M* NaF (pH = 5.2–10.8)			85	1980
(110)	100 m*M* KI			86	1980
(110)	20 m*M* NaF		No	87	1980
(110)	20 m*M* NaF pH = 5	−0.09 [a]	No	90	1980
(110)	20 m*M* NaF + diethylether		Yes	93	1981
(110)	20 m*M* NaF + 1 *M* diethylether		Yes	104	1982
(110)	10 m*M* NaF		No	94	1982
(110)	10 m*M* NaBr		Yes	95	1982
(110)	KI, KBr, KCl, NaF, K_2SO_4, $NaBF_4$			96	1983
(110)	200 m*M* K_2SO_4 + pyridine		Yes	97	1983
(110)	10 m*M* NaF + diethylether		Yes	98	1983

(continued on p 242)

TABLE 2 (continued)

Co in Miller indices	Solutions	E_{min} in the most dilute solution or pzc, vs SCE/V	Adsorption	Ref.	Year
(111)–(110) zone [d]					
4 faces	5–100 m*M* KCl		Yes	71	1973
3 faces	10 m*M* NaF		No	79	1976
4 faces	100 m*M* KI		Yes	80	1978
5 faces	10 m*M* NaF		No	94	1982
2 faces	10 m*M* NaBr		Yes	95	1982
(111)–(100) zone [d]					
(211)	10 m*M* KBr		Yes	70	1971
2 faces	10 m*M* NaF		No	79	1976
3 faces	100 m*M* KI		Yes	80	1978
6 faces	10 m*M* NaF		No	94	1982
3 faces	10 m*M* NaBr		Yes	95	1982
(311)	10–40 m*M* NaF, 20 m*M* NaF + 20 m*M* NaBr			96	1983
1 face	200 m*M* K_2SO_4 + pyridine			97	1983
(100)–(110) zone [d]					
3 faces	10 m*M* NaF		No	79	1976
4 faces	100 m*M* KI		Yes	80	1978
(210)	10–500 m*M* NaF		Slight	67	1982
(210)	10 m*M* $LiClO_4$		No	67	1982
4 faces	10 m*M* NaF		No	94	1982
2 faces	10 m*M* NaBr		Yes	95	1982
(210)	KI, KBr, KCl, NaF, $HClO_4$			96	1983

[a] E_{min} is said to coincide with the pzc
[b] Mono-oriented polycrystalline gold
[c] Mono-oriented polycrystalline gold and conventional crystal
[d] Faces of high indices

observed, then the shape of the capacity peaks and the reproducibility of the $C(E)$ curves are used to check the cleanness of the interface.

The differences observed between the $C(E)$ curves of the three faces of simplest indices in sulphate aqueous solutions in 1967 [11] suggested further experimental work [12–14,29,67–100].

A general survey of the published results concerning the dl on gold is given Table 2. It can be seen that at the beginning only the three faces of simplest indices were studied, but as soon as 1973 results for *faces of higher indices* were published, their co are on the three main zones of the projected unit stereographic triangle. Although it is now clearly understood, following either the bond-order notation [32] or the TLK model [33], that on two zones there is a "turning-point": (311) and (210) and therefore five sections should be considered (Fig. 9) [96], the results are given in three groups corresponding to the three zones, besides (111), (100) and (110).

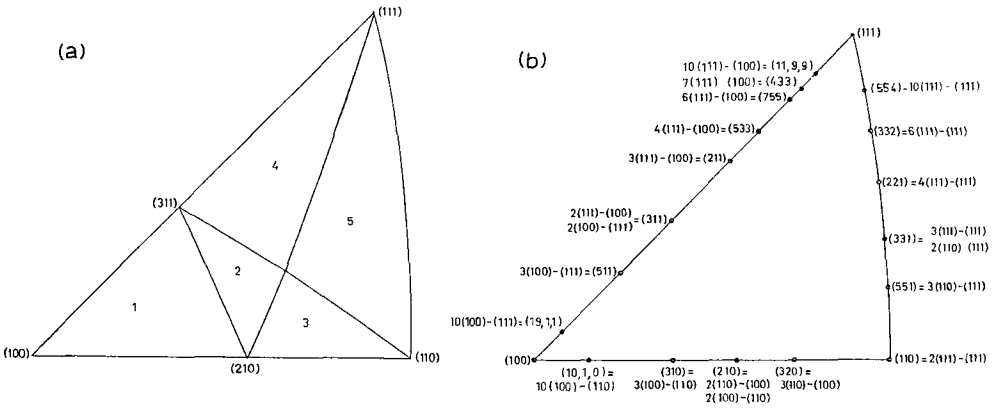

Fig. 9. Unit stereographic triangle for fcc structure with the (100) face at the centre of the projection. (a) Regions which correspond to different bond orders [32].

Region	1	2	3	4	5
Bond order	abcdef	abcedf	abcefd	abecdf	abecfd

(b) Accepting the notation of Lang et al [33] $n(h_t k_t l_t)-(h_s k_s l_s)$ where $(h_t k_t l_t)$ represents the terrace, $(h_s k_s l_s)$ represents the step face and n measures the width of terrace in number of atoms

Although the influence of the co was first clearly demonstrated for gold in cases where there is adsorption [11–14], early attention was paid to results in dilute NaF assuming no specific adsorption [69]. It was shown that as soon as there is no disturbed layer at the surface, the pzc observed does not depend on the surface preparation (conventional single-crystal face or vaporized film) [18,19], but could be drastically changed by fast cycling of the explored potential range which changes the relief of the surface [77]. But as "secondary effects" were observed for the three faces of simplest indices, at the same period, for clarity we will describe them first.

These "secondary effects", i.e.

—for the (100) gold face [72,73], influence of the negative limit of the explored range of potential on the pzc and on the hysteresis existing between the both sweeps of the $C(E)$ curves (summarized in ref. 96);

—for the (111) gold face [72,76,80,86], hysteresis of the $C(E)$ curves in a smaller range of potential (summarized in ref. 96);

—for the (110) gold face [75,80,95], appearance of a frequency-dispersive peak on the $C(E)$ curves (summarized in ref. 96);

were tentatively explained by reconstruction of the first layer of atoms of the surface at the electrochemical interphase [96] as observed in vacuum. These reconstructions which probably cause part of the frequency dispersion observed for the $C(E)$ curves made the analysis of the experimental results obtained for gold faces extremely difficult. These reconstructions exist less and less as the face is further removed from the simple index face.

As the "frequency dispersion" of the $C(E)$ curves has been mentioned, it is better

to discuss this point now. For all published results to date, frequency dispersion is much larger for gold faces than for silver for instance. Recently, for (210) in NaF (Fig. 8) and (100) in $LiClO_4$ [99] no frequency dispersion (from 15 to 80 Hz) was observed, but only in a short range of potential (0.4 V); at more positive potentials there is probably the beginning of the oxidation of gold and at more negative potentials there is the beginning of the reduction of the solvent. However, in some cases, when there is adsorption, frequency dispersion was $< 6\%$ (from 12 to 60 Hz) (Fig. 10 of ref. 96). This explains why quantitative analysis of the results obtained was not tried.

Despite these difficulties, a wealth of new information has been obtained from gold electrodes. First, without specific adsorption, although it was shown that there is probably a slight adsorption of the fluoride ion [67,99] *the set of pzc* determined in dilute NaF describes clearly the influence of the co. Comparison with electronic work functions of the same faces was possible only for neighbouring faces of (111) [94], but was possible with electronic work function of faces of another fcc metal: copper [101]. Figure 10 was drawn from the values of ref. 94 taking into account the fact that, for crystallographers, the main zones can be only represented two by two on one straight line. Comparison with another parameter [79]: the relative surface energy γ (*hkl*) [taking as an arbitrary unit $\gamma_{(210)}$] calculated using as an approximation only nearest-neighbour interactions, is surprisingly good; $\gamma_{(311)}$ and $\gamma_{(210)}$ were put in coincidence with their pzc as these two faces are said to be unreconstructed. Obviously, five sections appear on the curve: (210) and (311) are "turning-points" and there are cusps for (111) and (100). This demonstrates that the atomic arrangement at the surfaces of the faces, at the pzc, is not far from that of a just truncated crystal.

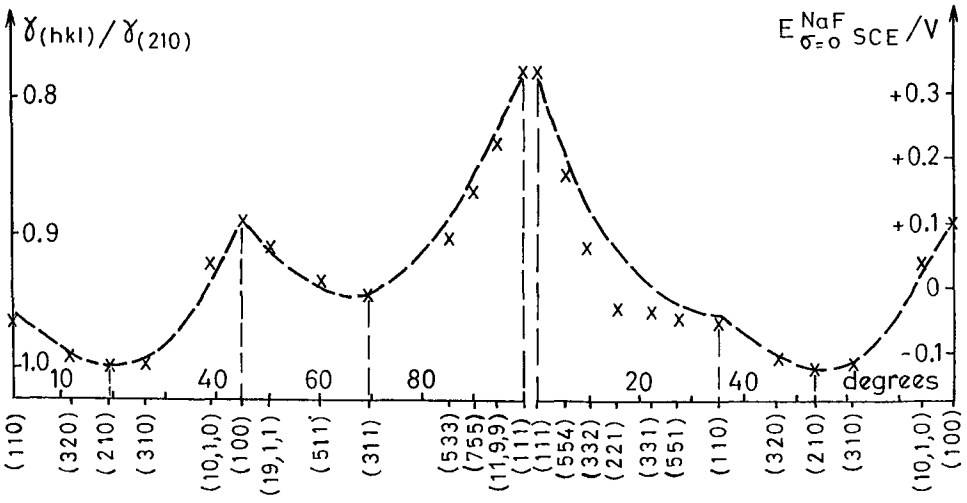

Fig 10 Variation of the relative surface energy (— — —) [79] and pzc [94] of gold faces in 10 m*M* NaF at room temperature with crystallographic orientation. Here (*hkl*) is a family of planes.

The E_{min} of polycrystalline gold was found close to those of the (110) and (410) faces between -0.05 and -0.08 V [102,103].

Determination of the variations of the *inner-layer capacity* (C^i) with respect to the density of charge at the electrode surface (σ) was attempted for gold faces. The pattern of the curve is the same as for silver faces. For (210) [67] a slightly asymmetrical curve and a maximum close to zero charge density was found; but due to the frequency dispersion and the difficulty in determining the roughness factor this result is less reliable than for silver faces. For (100) [99] the pattern of the $C^i(\sigma)$ curve varies with the concentration of the solution as was observed for polycrystalline gold in perchloric acid [102]; this variation was not observed for polycrystalline gold in fluoride solutions [103].

Some optical measurements were carried out on gold faces. In situ electroreflectance on gold faces [29,81,90] has shown that at the electrochemical interface the (111) and (100) faces are isotropic with respect to the plane of polarization of the indicent light, while the (110) face is anisotropic. The apparent change in concentration of water is not the same when the electric vector of the plane polarized light is parallel or perpendicular to the atomic "rails" of the (110) face [29] (the symmetry of the (110) face still exists in aqueous solution, as was observed for silver [28] and copper [30]). This method allowed metallic surface states to be observed at the (100) face of gold in the dl region [64].

Surface plasmons (surface electromagnetic waves) were excited at the (111) face–aqueous solution interface with visible light using an attenuated total reflection arrangement and the dispersion curve was given [62].

When there is specific ionic adsorption on gold faces the problem becomes more complicated, because the strength of adsorption as well as its variation with charge

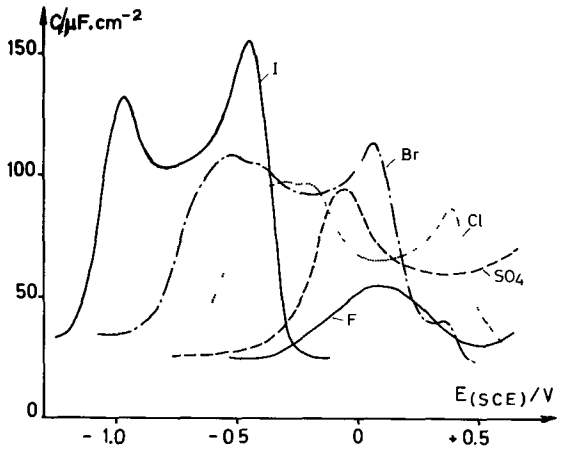

Fig. 11. $C(E)$ curves for the (110) face of gold in different media. 100 mM KI, KBr, KCl (80 Hz, 5 mV s^{-1} [70–73], 200 mM K_2SO_4 (130 Hz, 100 mV s^{-1}) [12]; 500 mM NaF (20 Hz, 5 mV s^{-1}) [96].

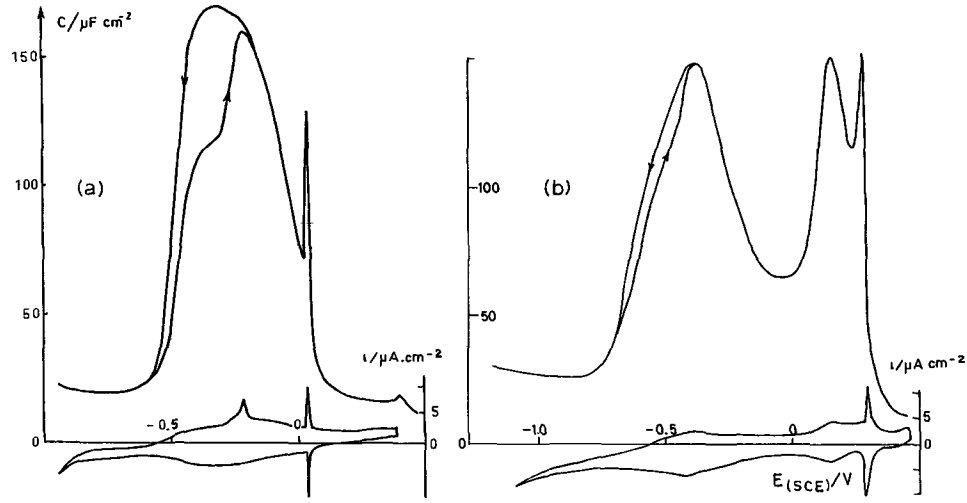

Fig. 12. $C(E)$ curves (20 Hz, 5 mV s^{-1}) and $i(E)$ curves (20 mV s^{-1})· (a) 100); (b) (311) gold faces, in 2 mM bromide solutions [70,96,100]

depends on the atomic structure of the gold surface. Quite distinctive patterns are observed for the $C(E)$ curves of each face. A general pattern can be discerned for: (100) (Fig. 5 of ref. 96); (110) (Fig. 11); (111) (see Fig. 1 of ref. 97); (210) (Fig. 11 of ref. 96); (311) (Fig. 9 of ref. 96). Frequently three capacity peaks are seen which shift towards negative potentials as the adsorbability increases. For some co they merge, then one can be only a shoulder on another (Fig. 12). This was also observed for silver, another fcc metal (Fig. 5).

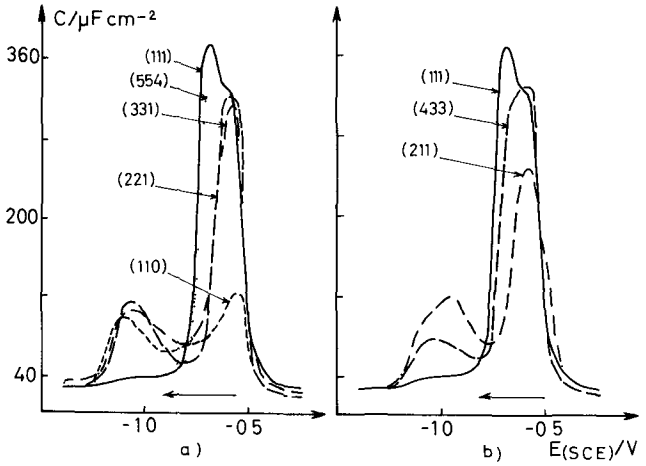

Fig 13. $C(E)$ curves for gold faces showing the systematic change of the amplitudes of the peaks with the crystallographic orientation for iodide ion adsorption (100 mM KI): (a) on the (111)–(110) zone; (b) from (111) towards (311) [80].

The patterns of the $C(E)$ curves of higher-index faces on the five sections of the three main zones are intermediary, and some regularities are observed. For the (111)–(110) zone, a systematic change of the $C(E)$ curves was first observed for chloride adsorption [71], then for iodide adsorption [80] (Fig. 13a): the peak at the most negative potentials appears as the monoatomic step density increases when the co goes towards (110) from (111); at the same time the large capacity peak of (111) decreases in area. This is also true for the (111)–(311) section for iodide adsorption (Fig. 13b) and bromide adsorption [100]. For the three other sections systematic changes are also observed [100], although the secondary effects exist. A full analysis of these $C(E)$ curves is hampered by the difficulty of carrying out quantitative analysis for gold electrodes, but comparable regularities occur in the deposition of submonolayer amounts of Pb on the same gold faces [26,89].

Comparison with the analysis carried out for silver faces gives us a clue to the understanding of $C(E)$ curves for ionic adsorption on gold faces. From the quantitative analysis of adsorption of chloride ion on Ag(110) (Fig. 4 of ref. 49) (which exhibits a general pattern similar to Au(110) [75,80,95,96]), we know that the peak at the most negative potentials is related to the peak of the inner-layer capacity without adsorption ascribed to reorientation of water (this is also clear from the study of pyridine adsorption on Au(110) [97]). The middle peak is an ionic adsorption peak related to the inflection in the adsorption isotherm. The narrow peak at the most positive potentials seems to be connected to partial charge transfer. The three peaks are also seen for (311) (Fig. 12b). For Ag(210) and Au(210) the general patterns are similar (Fig. 15 of ref. 49). For Ag(100) two peaks merge together (Fig. 5), similarly for Au(100) [72,73,80,96] (Fig. 12a). Sometimes only a broad peak is observed. For Ag(111) (Fig. 4 of ref. 49), the three peaks are mixed, but for Au(111) a huge double peak is systematically observed [72,76,80,96,97] which was not clearly explained.

As early as 1968 results for the *adsorption of a neutral organic substance* (pyridine) on gold faces were published [13,14]; recently these results have been explained by coadsorption with the anion of the base electrolyte and reconstruction of the (100) face [97]. For another neutral organic substance (diethylether), qualitative results obtained by a potentiodynamic method were published [93,104], and a quantitative analysis was then carried out for results obtained by a chronocoulometric method [98]; energies of adsorption were calculated and other parameters of the Frumkin adsorption isotherm were given. By the chronocoulometric method, these measurements were obtained on probably reconstructed faces.

(III.3) Copper

Copper belongs to the first group of the periodic table. Its electronic structure is $(3d^{10})\ 4s^1$. It crystallizes in the fcc system and its melting-point is 1083°C.

The crystals were grown either by zone melting, or pulling a seed from a melt or by the Bridgman method [105].

The copper single-crystal electrode surfaces were prepared by electropolishing in

phosphoric acid followed by electrochemical reduction of the electrode. The isolation of the faces of interest was carried out with the aid of Teflon holders [105,106] or by masking with polystyrene [107].

The pzc of copper single-crystal faces was determined using the minimum of $C(E)$ curves in dilute solutions of NaF [105,106,108,109] or estimated from the position of the adsorption–desorption peak at negative potentials on the $C(E)$ curves in the presence of tetrabutylammonium cation [110].

It is clear from Table 3 that, as for the other fcc metals, in the case of copper the more close packed the face, the more positive is the value of the pzc [110]. It has been suggested [110] that the more positive values obtained earlier [105,106,108] must be connected with oxidation of the copper electrode. It could also explain discrepancies of E_{min} for polycrystalline copper [106,111].

Capacitance measurements in solutions containing organic compounds have shown that benzotriazol and naphthalene are more strongly adsorbed on the (110)

TABLE 3

Data obtained on copper faces

Co in Miller indices	Solutions	E_{min} in the most dilute solution or pzc, vs SCE/V	Adsorption	Ref.	Year
(111)	7–50 mM NaF	−0.255 [a]	No	106	1972
(111)	50 mM Na_2SO_4 + benzotriazol		Yes	112	1972
(111)	10–50 mM NaF	−0.265 [a]	No	105	1973
(111)	7–800 mM NaF	−0.265 [a]	No	108	1975
(111)	50 mM Na_2SO_4 + TBA^+		Yes	107	1977
(111)	50 mM Na_2SO_4 + $(NH_2)_2CS$		Yes	107	1977
(111)	10–800 mM NaF	−0.165 [a]	No	109	1978
(111)	50 mM Na_2SO_4 + TBA^+	−0.57 ± 0.02 [b]	Yes	110	1979
(100)	7–50 mM NaF	−0.290 [a]	No	106	1972
(100)	7–50 mM NaF	−0.290 [a]	No	105	1973
(100)	7–800 mM NaF	−0.29 [a]	No	108	1975
(100)	50 mM Na_2SO_4 + TBA^+		Yes	107	1977
(100)	10–800 mM NaF	−0.29 [a]	No	109	1978
(100)	50 mM Na_2SO_4 + TBA^+	−0.70 ± 0.05 [b]	Yes	110	1979
(110)	7–100 mM NaF	−0.315 [a]	No	106	1972
(110)	7–100 mM NaF	−0.365 [a]	No	106	1972
(110)	50 mM Na_2SO_4 + benzotriazol		Yes	112	1972
(110)	7–10 mM NaF	−0.315 [a]	No	105	1973
(110)	7–50 mM NaF	−0.365 [a]	No	105	1973
(110)	7–800 mM NaF	−0.365 [a]	No	108	1975
(110)	50 mM Na_2SO_4 + TBA^+		Yes	107	1977
(110)	10–800 mM NaF	−0.365 [a]	No	109	1978
(110)	5 mM Na_2SO_4 + TBA^+	−0.87 ± 0.05 [b]	Yes	110	1979

[a] E_{min} is said to coincide with the pzc

[b] Pzc obtained by an indirect method.

face than on the (111); the adsorption behaviour of the polycrystalline copper electrode is in between those of the (111) and (110) faces [112].

Adsorption of thiourea, *n*-propanol and tetrabutylammonium (TBA^+) cation in sulphate base solution was investigated on faces of simple indices of copper

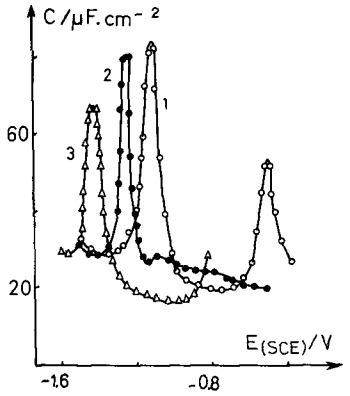

Fig. 14. $C(E)$ curves for copper faces in 50 mM Na_2SO_4 + 5 mM TBAI· (1) (111); (2) (100), (3) (110) [107].

[107,110]. In solutions containing thiourea, chemisorption was observed on the polycrystalline electrode but not on the single-crystal face [107].

It can be seen from Fig. 14 that with increasing reticular density of the faces the adsorption–desorption peak at negative potentials for TBA^+ shifts to more positive potentials; this is related to the crystallographic effect of the pzc of the faces [110]. The difference of the peak potentials for the (111) and (110) faces is about 0.3 V and this corresponds [105] to the difference of the electronic work functions of these faces.

In situ electroreflectance on copper faces has shown that, at the electrochemical interface in sulphuric acid, all faces are anisotropic with respect to the plane of polarization of the incident light, except for (100), (111), (211) and some neighbouring faces of (111) [30].

The major experimental difficulty for copper faces is the great tendency of the electrode surface to oxidize; this explains some discrepancies among published data.

(III.4) Zinc

Zinc crystallizes in the hcp system. Its electronic structure is $4s^2$. Its melting-point is 419.4°C.

In refs. 113–115 the basal face (0001) was prepared by cleavage of a single crystal at the temperature of liquid nitrogen, the prismatic face $(10\bar{1}0)$ anf the face $(11\bar{2}0)$ were cut and prepared by polishing in nitric acid. The precision of the orientations of the faces in the latter case was about 2–3°. The isolation of the face of interest was achieved using polystyrene dissolved in toluene.

The first attempt to determine the pzc of a single-crystal sp metal by $C(E)$ curves in dilute solutions was made on zinc [2,3]. In these works it was found that the pzc of the (0001) face is ~ 80 mV more positive than the pzc of the $(10\bar{1}0)$ face which is less densely packed at the surface; E_{min} for the polycrystalline zinc was found to be in between these pzcs, at about −0.84 V.

Later [6,116] it was pointed out that the determination of the pzc by direct observation of the minimum on the $C(E)$ curve in dilute solutions is not possible for zinc, because this potential is close to the reversible standard potential of zinc in aqueous solutions. In more recent work [117,118] it was found that E_{min} for a polycrystal is more negative, about −1.14 V.

More reliable values of the pzc of zinc single-crystal faces [119] were obtained from the dependence of the potential of the desorption peak at negative potential with varying concentration of base electrolyte. The values of the pzc are given in Table 4. It is obvious that the pzc of the basal face is more positive than those of the other two faces. Most of the investigations on zinc crystal faces were made in solutions containing organic substances: tetraalkylammonium [6], ethylenediamine [120], hexanol [113,121,122], tetrabutylammonium [113–115,122,123], camphor [122,124], cyclohexanol [123,125,126] and thiourea [127–129]. For all these substances, dependence of adsorption properties on co was observed. This dependence was clearly demonstrated when it was possible to observe adsorption–desorption peaks on the $C(E)$ curves. These peaks—in the same conditions—shift to more negative potentials in the order (0001), $(10\bar{1}0)$, $(11\bar{2}0)$ and this corresponds to the

TABLE 4

Data obtained on zinc faces

Co in Miller indices	Solutions	E_{min} in the most dilute solution or pzc, vs SCE/V	Adsorption	Ref	Year
(0001)	10 mM $Na_2SO_4 + H_2SO_4$ (or NaOH)	−0.84 [a]	No	2	1956
(0001)	10 mM $Na_2SO_4 + H_2SO_4$	−0.84 [a]	No	3	1957
(0001)	5–250 mM $H_2SO_4 + Na_2SO_4$ (pH 2.87 and 2.96)	+0.84 [a]	No	2	1957
(0001)	100–1000 mM KCl	−0.89 [b]	Yes	6	1960
(0001)	KCl, KI + $(C_4H_9)_4^+$		Yes	6	1960
(0001)	5–1000 mM $NaClO_4$	−1.14 [a]	No	117	1969
(0001)	500 mM Na_2SO_4 + ethylenediamine		Yes	120	1970
(0001)	10 mM KBr + hexanol		Yes	113	1972
(0001)	100 mM KI + TBAI		Yes	114	1972
(0001)	10–100 mM KBr + hexanol		Yes	121	1972
(0001)	5 mM Na_2SO_4 + hexanol (saturated)		Yes	121	1972
(0001)	100–300 mM KCl	−1.01 [b]	No	124	1974
(0001)	NaF + camphor, KCl + n-amyl alcohol		Yes	124	1974

TABLE 4 (continued)

Co in Miller indices	Solutions	E_{min} in the most dilute solution or pzc, vs. SCE/V	Adsorption	Ref.	Year
(0001)	10 m*M* KBr + aniline		Yes	122	1974
(0001)	10 m*M* KBr + hexanol		Yes	122	1974
(0001)	100 m*M* KI + camphor (saturated), TBAI		Yes	122	1974
(0001)	100 m*M* KCl(H_2SO_4) + cyclohexanol		Yes	125	1975
(0001)	50 m*M* Na_2SO_4 (or KI) + TBA^+		Yes	115	1975
(0001)	300 m*M* KCl	−1.01 [b]	No	123	1975
(0001)	100 m*M* KCl	−1.00 [b]	No	123	1975
(0001)	100 m*M* KCl + cyclohexanol		Yes	123	1975
(0001)	100 m*M* KI + TBAI		Yes	123	1975
(0001)	100 m*M* KCl + *n*-amyl alcohol		Yes	123	1975
(0001)	100 m*M* KCl (H_2SO_4) + cyclohexanol		Yes	126	1975
(0001)	NaF or KCl thiourea, *n*-amyl alcohol, camphor	−0.99, −1.01 [b]	Yes	127	1976
(0001)	100 m*M* KCl (pH 3.7) + 0.6–300 m*M* thiourea		Yes	128	1980
(0001)	10–300 m*M* KCl (pH 3.7) + thiourea		Yes	129	1980
$(10\bar{1}0)$	10 m*M* Na_2SO_4 ($+H_2SO_4$)	−0.92 [b]	No	3	1957
$(10\bar{1}0)$	500 m*M* Na_2SO_4 + ethylenediamine		Yes	120	1970
$(10\bar{1}0)$	210 m*M* NaF + camphor	−1.16 [b]	Yes	124	1974
$(10\bar{1}0)$	50 m*M* Na_2SO_4 (or KI) + TBA^+		Yes	115	1975
$(10\bar{1}0)$	200 m*M* KCl	−1.07 [b]	No	123	1975
$(10\bar{1}0)$	100 m*M* KCl + cyclohexanol		Yes	123	1975
$(10\bar{1}0)$	100 m*M* KCl (H_2SO_4) + cyclohexanol		Yes	126	1975
$(10\bar{1}0)$	KCl or NaF + thiourea, *n*-amyl alcohol, camphor	−1.07, −1.08 [b]	Yes	127	1976
$(11\bar{2}0)$	100 m*M* KI + TBAI		Yes	122	1974
$(11\bar{2}0)$	50 m*M* Na_2SO_4 (or KI) + TBA^+		Yes	115	1975
$(11\bar{2}0)$	200 m*M* KCl	−1.12 [b]	No	123	1975
$(11\bar{2}0)$	3 m*M* KCl	−1.10 [b]	No	123	1975
$(11\bar{2}0)$	100 m*M* KI + TBAI		Yes	123	1975
$(11\bar{2}0)$	100 m*M* KCl(H_2SO_4) + cyclohexanol		Yes	126	1975
$(11\bar{2}0)$	3 m*M* KCl (pH 3.7)	−1.09 [a]	No	127	1976
$(11\bar{2}0)$	100 m*M* KCl + *n*-amyl alcohol, thiourea	−1.08, −1.10 [b]	Yes	127	1976
$(11\bar{2}0)$	NaF (dif. conc.) + camphor	−1.08, −1.10 [b]	Yes	127	1976
$(11\bar{2}0)$	100 m*M* KCl (pH 3.7) + thiourea		Yes	128	1980

[a] E_{min} is said to coincide with the pzc.
[b] Pzc obtained by an indirect method

shift of potential of the pzc of the three faces to the negative potentials. It is mentioned [115] that the height of the peaks decreases in the same sequence; this is said to be connected with the increase of water adsorption energy on the faces. As an

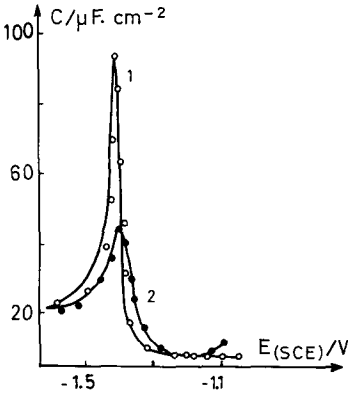

Fig. 15 $C(E)$ curves for zinc in 100 mM KCl + 150 mM cyclohexanol· (1) (0001) face, (2) polycrystal [130].

example, the $C(E)$ curves for the (0001) face in solution containing cyclohexanol [130] are given in Fig. 15. As can be seen, the peaks on the single-crystal faces are narrower and higher than the peaks on the polycrystal. Splitting of the adsorption–desorption peak was observed for the first time on the polycrystalline Zn electrode; this was explained by the presence of different faces at the surface [114,122].

(III.5) Lead

Lead crystallizes in the fcc system. Its electronic structure is $6s^26p^2$. Its melting-point is 327°C.

The preliminary surface preparation includes electrochemical polishing and electroreduction of the surface. The measurements were carried out on electrodes embedded in Teflon holders.

The first attempts to determine the pzc of separate faces of lead was made using $C(E)$ curves in dilute solutions of NaF and Na_2SO_4 [131]; this work also deals with polycrystalline lead. On the $C(E)$ curves at the minimum, the frequency dispersion was about 10% from 210 to 1010 Hz. The values of the potential of the minima of the $C(E)$ curves, determined in 10 mM NaF and Na_2SO_4 solutions, are given in Table 5. It is clear that the influence of co on the pzc is very small, not more that 40 mV: the pzc of the polycrystalline lead is near the pzc of the separate faces [131,132]. In sulphate solutions E_{min} is shifted by 30 mV, and as it seems that specific adsorption of this anion does not take place on lead, this shift could be connected to the asymmetric properties of this electrolyte.

On the same faces, investigation of organic adsorption: hexanol, TBAI, camphor,

TABLE 5

Data obtained on lead faces

Co in Miller indices	Solutions	E_{min} in the most dilute solution or pzc, vs. SCE/V	Adsorption	Ref.	Year
(111)	10 m*M* NaF	-0.86 ± 0.01 [a]	No	131	1978
(111)	5 m*M* Na_2SO_4	-0.89 ± 0.01	No	131	1978
(111)	50 m*M* Na_2SO_4 + cyclohexanol		Yes	133	1980
(111)	50 m*M* Na_2SO_4 + propyl acetate		Yes	134	1981
(111)	100 m*M* KI + TBAI		Yes	134	1981
(100)	10 m*M* NaF	-0.83 ± 0.01 [a]	No	131	1978
(100)	5 m*M* Na_2SO_4	-0.85 ± 0.01	No	131	1978
(100)	50 m*M* Na_2SO_4 + cyclohexanol		Yes	133	1980
(100)	100 m*M* KI + TBAI		Yes	134	1981
(110)	10 m*M* NaF	-0.82 [a]	No	131	1978
(110)	5 m*M* Na_2SO_4	-0.85	No	131	178
(110)	50 m*M* Na_2SO_4 + cyclohexanol		Yes	133	1980
(112)	10 m*M* NaF	-0.82 [a]	No	131	1978
(112)	5 m*M* Na_2SO_4	-0.85	No	131	1978
(112)	50 m*M* Na_2SO_4 + cyclohexanol		Yes	133	1980
(112)	100 m*M* KI + TBAI		Yes	134	1981
(112)	50 m*M* Na_2SO_4 + propylacetate		Yes	134	1981

[a] E_{min} is said to coincide with the pzc.

methylbutyl ketone and propylacetate was studied [133,134]. Adsorption of cyclohexanol and TBAI on the (111) face differs slightly from adsorption on the other faces and on a polycrystalline electrode, this is said to be connected with the more pronounced hydrophilicity of this face. Splitting of the adsorption–desorption peak was observed on the polycrystalline electrode and in some cases at the (100) and (112) faces in solutions containing TBAI or propylacetate [134]. This phenomenon—as in the case of zinc (see section III.4) and bismuth (see section III.7)—was explained by the presence of different crystallographic planes at the surfaces examined.

(III.6) Tin

Tin crystallizes in the tetragonal system. Its electronic structure is $5s^25p^2$. Its melting-point is 231.8°C.

The three faces studies, (001), ($\bar{1}$10) and (110), were electropolished and thoroughly rinsed in deoxygenated, acidified, dilute sulphate solution before the experiments [135]. Data obtained with tin faces are given in Table 6.

Sulphate ions do not adsorb on tin faces. In dilute sulphate solutions the pzc does not vary with co; this seems connected to the low melting-point and hence higher mobility of the surface atoms.

TABLE 6

Data obtained on tin faces

Co in Miller indices	Solutions	E_{min} in the most dilute solution or pzc, vs. SCE/V	Adsorption	Ref	Year
(001)	1.5–50 mM Na_2SO_4	-0.60 ± 0.01 [a]	No	135	1981
(001)	200 mM KI + TBAI		Yes	135	1981
(001)	50 mM Na_2SO_4 + cyclohexanol		Yes	135	1981
(001)	50 mM Na_2SO_4 + aniline phenol		Yes	136	1982
($\bar{1}10$)	1.5–50 mM Na_2SO_4	-0.60 ± 0.01 [a]	No	135	1981
(110)	1.5–50 mM Na_2SO_4	$+0.61 \pm 0.01$ [a]	No	135	1981

[a] E_{min} is said to coincide with the pzc.

For halides, the order of increasing adsorption is $F^- < Cl^- < Br^- < I^-$, as for other sp metals.

The $C(E)$ curves for adsorption of TBAI on the (001) face and a polycrystalline electrode (Fig. 3 of ref. 135) suggest an anisotropy of the adsorption of organic substances; but from the coincidence of the surface pressure vs. potential curves—for the (001) face and the polycrystalline electrode—for adsorption of aniline and phenol, this anisotropy would be very weak [136].

Adsorption parameters were calculated for adsorption of cyclohexanol on the (001) face [135].

(III.7) Bismuth

Although bismuth is considered as a semi-metal, we analyse the published data here. Bismuth crystallizes in the rhombohedral system. Its electronic structure is $6s^2 6p^3$. Its melting-point is 271°C.

The isolation of the faces was made by a thin polystyrene film (dissolved in toluene) covering the part of no interest and then the sample was placed in a Teflon holder. Before measurements, electrodes were electrochemically polished and thoroughly rinsed. Some work was carried out in surface-inactive electrolytes [137,138]. The pzc and the dl structure were studied using $C(E)$ curves; the frequency dispersion of the capacitance values was 2–3% from 110 to 2000 Hz. The results in dilute solutions of potassium fluoride and potassium sulphate for E_{min} are given in Table 7. The anisotropy of the pzc is < 100 mV, and this is in good agreement with the small anisotropy of the work function for bismuth [137]. For polycrystalline bismuth E_{min} was found at -0.63 V [139].

In these papers the value of the slopes (f) of the Parsons–Zobel plots are discussed. In ref. 138 it is said that $1/C - 1/C^d$ varies linearly in KF from 1 to 100 mM, but that the slope depends on the co; f for ($01\bar{1}$) and ($2\bar{1}\bar{1}$) is 1.1 and this value was attributed to the difference between true and geometric areas, the larger value of

TABLE 7

Data obtained on bismuth faces

Co in Miller indices	Solutions	E_{min} in the most dilute solution or pzc, vs. SCE/V	Adsorption	Ref	Year
(111)	2.5–50 m*M* KF	−0.65 [a]	No	137	1974
(111)	5–100 m*M* K_2SO_4	−0.68 [a]	No	137	1974
(111)	2 m*M* KF + KCl, KBr, KI		Yes	137	1974
(111)	500 m*M* Na_2SO_4 + methylbutyl ketone, propylacetate		Yes	143	1975
(111)	(500 − *x*) m*M* KF + *x* m*M* KI (*x* = 0–500)		Yes	140	1975
(111)	100 m*M* $NaF(HClO_4)$ + camphor		Yes	149	1978
(111)	50 m*M* $Na_2SO_4(H_2SO_4)$ + *n*-butanol		Yes	148	1978
(111)	100 m*M* $KF(H_2SO_4)$ + cyclohexanol		Yes	145	1978
(111)	100 m*M* NaF + camphor		Yes	150	1979
(111)	100 m*M* $NaF(HClO_4)$ + camphor		Yes	151	1979
(111)	100 m*M* $NaF(HClO_4)$ + cyclohexanol		Yes	151	1979
(111)	(100 − *x*) m*M* KF + *x* m*M* KI (*x* = 0–100)		Yes	141	1980
(111)	100 m*M* NaF + camphor		Yes	152	1980
(111)	25 m*M* Na_2SO_4 (or H_2SO_4) + cyclohexanol		Yes	147	1981
(111)	25 m*M* K_2SO_4 + coumarine		Yes	155	1981
(111)	13–100 m*M* $LiClO_4$ (in ethanol)	−0.48 ± 0.01 [a]	Yes	157	1981
(111)	300 m*M* KF + thiourea		Yes	153	1982
(111)	100 m*M* KF + aniline		Yes	154	1982
$(01\bar{1})$	5 m*M* KF	−0.60 [a]	No	138	1977
$(01\bar{1})$	2 m*M* KF + KCl, KBr, KI		Yes	138	1977
$(01\bar{1})$	50 m*M* Na_2SO_4 + *n*-butanol		Yes	148	1978
$(01\bar{1})$	100 m*M* $KF(H_2SO_4)$ + cyclohexanol		Yes	145	1978
$(01\bar{1})$	*x* m*M* KI + (100 − *x*) m*M* KF (*x* = 0–100)		Yes	141	1980
$(01\bar{1})$	25 m*M* Na_2SO_4 (or H_2SO_4) + cyclohexanol		Yes	147	1981
$(01\bar{1})$	25 m*M* K_2SO_4 + coumarine		Yes	155	1981
$(01\bar{1})$	300 m*M* KF + thiourea		Yes	153	1982
$(01\bar{1})$	100 m*M* KF + aniline		Yes	154	1982
$(2\bar{1}\bar{1})$	5 m*M* KF	−0.57 [a]	No	138	1977
$(2\bar{1}\bar{1})$	2 m*M* KF + KCl, KBr, KI		Yes	138	1977
$(2\bar{1}\bar{1})$	50 m*M* Na_2SO_4 + *n*-butanol		Yes	148	1978
$(2\bar{1}\bar{1})$	100 m*M* $KF(H_2SO_4)$ + cyclohexanol, *n*-propanol		Yes	146	1978
$(2\bar{1}\bar{1})$	100 m*M* NaF + camphor		Yes	150	1979
$(2\bar{1}\bar{1})$	100 m*M* NaF + camphor		Yes	152	1980
$(2\bar{1}\bar{1})$	*x* m*M* KI + (100 − *x*) m*M* KF (*x* = 0–100)		Yes	141	1980
$(2\bar{1}\bar{1})$	25 m*M* Na_2SO_4 (or H_2SO_4) + cyclohexanol		Yes	147	1981
$(2\bar{1}\bar{1})$	300 m*M* KF + thiourea		Yes	153	1982
$(2\bar{1}\bar{1})$	100 m*M* KF + aniline		Yes	154	1982

[a] E_{min} is said to coincide with the pzc.

$f = 1.25$ for (111) has not yet been explained.

The variations of the inner-layer capacity with the charge density ($C'(\sigma)$) [138] for the different faces and for the polycrystalline electrode are given in Fig. 16. At significantly negative charges C' depends very little on the co. In the region of the pzc and for positive charges, C' decreases in the order: (111) > polyc > $(01\bar{1})$ > $(2\bar{1}\bar{1})$, and the hydrophilicity decreases in the same order [138]. In comparing the values of C', the values of the roughness factor f were not taken into account although they differ from unity.

The shifts of the E_{min} of the $C(E)$ curves were measured in KCl, KBr and KI solutions [137,138] and it was deduced that specific adsorption of halides on all the faces investigated and the polycrystalline electrode increases in the sequence $F^- < Cl^- < Br^- < I^-$. This order coincides with the sequence of increasing C' values at the pzc. Specific adsorption parameters were calculated [140,141] for bismuth crystal faces.

Recently, the behaviour of organic compounds has been studied on faces of bismuth: on the (111) face adsorption of methylbutylketone and polyacetate [142,143] and esters [144], on several faces adsorption of cyclohexanol and *n*-propanol [145–147], *n*-butanol [148], camphor [149–152], thiourea [153], aniline [154] and coumarine [155]. Adsorption of these substances was studied using $C(E)$ measurements at a given frequency of the ac signal. These curves have the usual form with sharp adsorption–desorption peaks. The height, number and position of these peaks depend on the co of the bismuth faces and also on the nature of the adsorbed organic substance. Adsorption parameters (interaction constants, equilibrium constant, etc.) were estimated from these $C(E)$ curves by the method of Frumkin and Damaskin [156]. It was shown that the adsorption parameters of polycrystalline spheres of bismuth are very close to those obtained for the (111) face; this fact confirms the idea that the (111) face predominates at the surface of polycrystalline bismuth spheres [146,148].

From the study of adsorption of thiourea [153], the order of "thiophilicity" for the faces of bismuth is $(01\bar{1})$ > $(2\bar{1}\bar{1})$ > (111), which is not the order of hydrophilicity [138]. The strength of adsorption of cyclohexanol and aniline on faces of

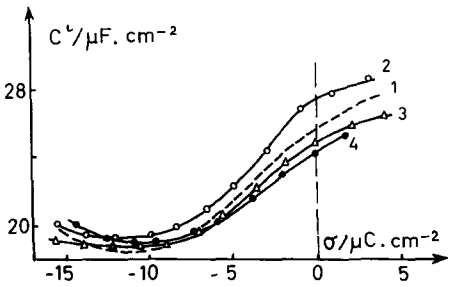

Fig. 16. $C'(\sigma)$ curves for bismuth in KF solution (1) polycrystal; (2) (111) face, (3) $(01\bar{1})$ face, (4) $(2\bar{1}\bar{1})$ face [138]

bismuth—from the variations of the potential at the maximum of the adsorption peaks with respect to the logarithm of the concentration—decreases as the thiophilicity; the reverse order is obtained for aniline from the height of the adsorption peaks. This last contradiction could be explained by competition of the interactions of the NH_2 groups and the π-electrons with faces of different hydrophilicity [154].

For faces of bismuth $C(E)$ curves were obtained in a non-aqueous solvent: ethanol with lithium perchlorate [157].

The data obtained for bismuth show that despite the small anisotropy of the pzc there is a strong dependence of the adsorption parameters on the co.

(IV) DISCUSSION AND COMPARISONS

(IV.1) Shortage of data

Although the experimental data on faces of different sp metals are numerous, for complete understanding of the influence of the co on the dl structure and properties some data are missing:

(a) Data were published for seven sp metals but no results concerning cadmium, indium, etc., are known.

(b) Only for gold were a large number of high-index faces studied. In order to obtain a general view of the influence of the co, it would be necessary to do this for other metals. Furthermore, it is probably not sufficient to study faces on the three main zones of the projected unit stereographic triangle as was done for gold.

(c) All measurements were carried out at room temperature. Temperature influence on the C^1 (σ) curves and the determination of the adsorption-excess entropies would be interesting.

(d) All experiments were carried out in aqueous solvent, except one paper for bismuth; it is obvious that measurements in organic solvents, non-polar solvents and molten salts would extend the understanding of the dl on sp metal faces.

(e) Most of the published data were obtained by $C(E)$ curves and only a few come from optical measurements; other methods, e.g. estance, modulation amplitude technique, or surface-enhanced Raman spectroscopy could provide a wealth of information.

(IV.2) Comparison of data on dl on faces

Although there are missing results, values already obtained can be compared. For all comparisons it must be kept in mind that reorganization of the faces could occur during electrochemical measurements, as the equilibrium established at the interface is not only electrostatic but also mechanical. Furthermore, for gold "reconstruction" was observed in solutions as it was in vacuum for 5d metals (Pt, Ir, Au) (see section III.2).

The succesful approach of dividing the solution side of the dl into two regions

defined in terms of the way in which the ions present interact with the electrode was possible for crystal faces of sp metals, although the division by a plane parallel to the electrode surface, the "outer Helmholtz plane" (oHp), is somewhat difficult to imagine in the case of solid surfaces.

(IV.2.1) The solution side of the oHp

Here, only long-range interactions obeying classical electrostatic laws exist. This results in dilute solutions with little or no adsorption—in a minimum on the $C(E)$ curves. To be observed clearly, this minimum has to occur in a range of potential where the interface is ideally polarizable. For a few faces this was not the case, for instance for the basal face of zinc. But for most of the faces studied the minimum was observed and was used to determine the pzc. The important point is that the different atomic structures of the faces give a different pzc. In view of the fact that the electronic work function is dependent on the co and the relation between the electronic work function and the pzc, this difference is not surprising. The parallelism observed for the pzc on gold faces and the calculated surface energies (Fig. 10), also exists for the electronic work function of another fcc metal, copper.

For all sp metals the *most densely packed face* presents the *most positive pzc* (except perhaps for lead), and the *roughest face*—on an atomic scale—the *most negative one* [respectively the (111) and (210) faces, for the fcc system]. *The difference between these pzc decreases with the melting-point of the metal*, from 0.460 V for gold to 0 V for tin, the surface atoms being more mobile close to the melting temperature.

(IV.2.2) The metal side of the oHp

Here, in the inner part of the dl, short-range interactions—as well as long-range interactions—exist. They change the solvent properties, and interactions between ions and metal which cannot be described by the Gouy–Chapman theory, take place.

(1) The water–metal interactions—as water is the only solvent used up to now—vary not only with the nature of the metal (the difference of hydrophilicity of the metals is well known), but with the co for one metal. The water–metal interactions in the case of no specific adsorption are described by the $C^1(\sigma)$ curves (Figs. 2 and 16). When there is specific adsorption, the contribution of the inner-layer capacity for a fixed amount of adsorbed ions ${}_{\sigma}C^1$ as a function of the electrode charge σ describes these interactions, as has been shown for silver faces.

(2) The metal–ion interactions. When they exist, the problem becomes more complicated because the strength of adsorption as well as its variation with charge depends on the atomic structure of the face. Quite distinctive patterns are observed for the $C(E)$ curves of each face. A general pattern can be discerned for one face of several metals, and this was shown for gold and silver (Figs. 5 and 12). Frequently three peaks are observed which shift towards negative potentials as the adsorbability of the anion increases. For some co they merge, then one can be only a shoulder on another (Figs. 5 and 12). For high-index faces on the five sections of the three main zones of the projected unit stereographic triangle, the patterns of the $C(E)$ curves

are in between, systematic changes being observed (Fig. 13): the influence of the monoatomic steps is clearly visible. The influence of atomic growth steps is also visible (Fig. 3).

Comparison of adsorption for different metals can be made only for metals which crystallize in the same system for the same co, in the same solution. The criterion for adsorption is either the disappearance, with increasing concentration, of the contribution of the diffuse part of the dl or the value of $\Delta E = \Delta\ (E_{\sigma=0,x} - E_{\sigma=0,y})$ (assuming no adsorption of y and x being the adsorbate).

(3) In the case of adsorption of organic substances (substitution of the solvent molecules by the organic substance in the inner part of the dl), if the range of potential in which the electrode is ideally polarizable is large enough, two adsorption–desorption peaks are observed on the $C(E)$ curves. But often only the more negative is observed, and this is the case of gold, bismuth and tin. Conversely, for silver, the two peaks were observed (Fig. 7). It was shown that this adsorption is sensitive not only to the co but also to growth steps which exist on the face (Fig. 7).

For silver, copper and bismuth the potential of the adsorption–desorption peak shifts with the co following the pzc of the faces; this was not observed for pyridine on gold faces.

Adsorption parameters were calculated for silver, gold, bismuth and tin faces; for gold and bismuth there is an influence of the crystallographic orientation.

At present it seems impossible to give a general view of the behaviour of the adsorption of organic substances on crystal faces.

(IV.3) Comparison with polycrystalline electrodes

Most of the studies of the dl on sp metals were achieved with polycrystalline metals, it is not within the scope of this paper to give their references. We will only discuss the ideas.

It has already been suggested that some of the difficulties encountered in quantitative analysis of $C(E)$ curves for these electrodes are connected with their crystallographic non-uniformity. The effect of this non-uniformity is difficult to predict. However, some models were proposed in which a weighted average of the three main co's was assumed to exist at the electrode surface; a qualitative coincidence was obtained between calculated and experimental $C(E)$ curves. This approach to polycrystalline surfaces may be wrong, because the difference in the surface energy of the crystal faces may produce a preferential orientation which is not accounted for in the model; furthermore, the extreme electrochemical behaviour of some defects or grains existing at the surface, can conceal the behaviour of others, although they exist and could be revealed by other methods.

For instance for polycrystalline gold and silver, on the $C(E)$ curves, the E_{min} was found close to the pzc of the (110) face; this was explained by the calculation of the weighted average of the three main co's. This is not a result of the prevailing contribution of this face to the polycrystalline surface, but could be due to the fact that the contribution of the diffuse part of the dl to the $C(E)$ curve is more clearly

expressed in the potential region of the pzc of the (110) face because of the low values of C of other faces in this region of potential.

It is easy to understand that for polycrystalline electrodes the roughness factor determined by the Parsons–Zobel plot is vitiated for the same reason. Roughness factors obtained by comparison of C values at very negative charge density with that of mercury (the roughness factor of which is unity) suffer from the assumption that all co's have the same value of C at this charge, which is not correct.

The $C(E)$ curves of polycrystalline surfaces—with no appearance of the contribution of the diffuse part of the dl—have been interpreted mostly as a superposition of the curves of the different faces.

In some studies the crystallographic non-uniformity of the polycrystalline surface has not been taken into account. Of course, for low-melting metals, for which little or no influence of the co is observed, this approach is reasonable. However, in explaining some experimental data for polycrystalline high-melting metals, it has been necessary to consider that the surface consists of a large amount of sufficiently small grains of different types. In this case, the polycrystalline electrode would exhibit a particular behaviour which may differ quantitatively from that of its crystal faces.

It is worth noting that all data for polycrystalline metals have been obtained with surfaces of unknown topography. Quantitative analysis of the results would require a complete description of the physical and chemical states of the surface, as well as a further study of grain boundaries, steps, terraces, defects, etc.

ACKNOWLEDGEMENT

The authors wish to express their gratitude to Dr. Roger Parsons for discussing this compromise of their different points of view.

LIST OF SYMBOLS

dl	electrochemical double layer
co	crystallographic orientation
pzc	potential of zero charge
$E_{\sigma=0}$	potential of zero charge
$C(E)$	differential capacity vs. potential
$i(E)$	direct current vs. potential
fcc	face-centered cubic
hcp	hexagonal close packed
E_{min}	potential at the minimum of the $C(E)$ curves
TLK	terraces, ledges, kinks
σ	charge density on the electrode
C^d	differential capacity of the diffuse part of the dl
C^i	differential capacity of the inner part of the dl
LEED	low-energy electron diffraction

$_{\sigma}C^{1}$	differential inner-layer capacity for a fixed amount of adsorbed ions
f	roughness coefficient

REFERENCES

1 A N. Frumkin, Eng. Exacten Naturwiss , 7 (1928) 270, J Res Inst. Catal. Hokkaido Univ., 15 (1967) 61
2 V L Heifetz and B.S. Krasikov, Dokl Akad Nauk., S S S.R , 109 (1956) 586; J. Phys Chem. (S.S.S.R.), 31 (1957) 1992.
3 B. Krasikov and V. Sisoeva, Dokl Akad Nauk, S.S S R., 114 (1957) 826
4 R P Johnson and W. Shockley, Phys. Rev., 49 (1936) 436
5 A Hamelin, Trait Surf , 10, No. 85 (1969) 15.
6 Tza Chuan-Sin and Z. Iofa, Dokl. Acad. Nauk, S S S.R., 131 (1960) 137.
7 R G. Rein, C.M. Shepcevich and R D. Daniels, J. Electrochem. Soc , 112 (1965) 739.
8 E. Sevastyanov and T. Vitanov, Elektrokhimiya, 3 (1967) 402.
9 G.M Schmid and N. Hackerman, J Electrochem. Soc., 109 (1962) 243.
10 G M. Schmid and N Hackerman, J. Electrochem Soc., 110 (1963) 440
11 J Clavilier, A Hamelin and G Valette, C R Acad Sci. (Paris), 265C (1967) 221.
12 A Hamelin, J. Clavilier and G. Valette, C.R. Acad Sci (Paris), 266C (1968) 435.
13 A Hamelin and G. Valette, C.R Acad. Sci. (Paris), 267C (1968) 127
14 A Hamelin and G Valette, C R. Acad. Sci (Paris), 267C (1968) 211
15 T H Grindstaff, U.S Energy Comm., TID 22 150 (1965) 129
16 A Chernov, E Guvargizov and H. Bagdasarov, Modern Crystallography, Vol. III, Crystal Growth, Moscow Science Ed , 1980
17 W. Bardsley, D I.J Hurle and J.E. Mullin, Crystal Growth. A Tutorial Approach, North-Holland, Amsterdam, 1979
18 J. Lecoeur, C Sella, L Tertian and A. Hamelin, C R Acad. Sci (Paris), 280 C (1975) 247
19 J Lecoeur, C. Sella and J.C. Martin, C.R Acad. Sci. (Paris), 287 C (1978) 447.
20 C. Nguyen Van Huong, R. Parsons, P Marcus, S Montes and J. Oudar, J. Electroanal. Chem., 119 (1981) 137
21 E Budevski, W Bostanov, T. Vitanov, Z Stoinov, A. Kotzeva and R. Kaishev, Elektrokhimiya, 3 (1967) 856.
22 R. Kaishev, G Blisnakov and A. Scheludko, Ber. Bulg Akad. Wiss. Phys. Ser , 1 (1950) 147.
23 E. Budevski and W. Bostanov, Electrochim. Acta, 9 (1964) 477.
24 E. Budevski, W Bostanov, T. Vitanov, Z. Kotzeva and R. Kaishev, Phys Stat. Sol., 13 (1966) 577, Electrochim. Acta, 11 (1966) 1697
25 T Vitanov and A. Popov, Trans S A.E S T , 10 (1975) 5.
26 A Hamelin and A Katayama, J. Electroanal. Chem , 117 (1981) 221.
27 T. Vitanov and A. Popov, to be published.
28 T.E. Furtak and D.W Lynch, J. Electroanal. Chem., 79 (1977) 1.
29 C Hinnen, C. Nguyen Van Huong, A. Rousseau and J.P Dalbera, J. Electroanal Chem., 106 (1980) 175.
30 R. Kotz and H.J Lewerenz, Surf Sci , 78 (1978) L233
31 J. Friedel, Les Dislocations, Gauthier-Villars, Paris, 1956, p. 135
32 J.F Nicholas, An Atlas of Models of Surfaces, Gordon and Breach, New York, 1965.
33 B. Lang, R.W. Joyner and G A. Somorjai, Surf. Sci., 30 (1972) 454.
34 E. Budevski, T. Vitanov, E S. Sevastyanov and A. Popov, Elektrokhimiya, 5 (1969) 90
35 G. Valette and A. Hamelin, C.R Acad. Sci. (Paris), 272C (1971) 602.
36 E S. Sevastyanov, T. Vitanov and A Popov, Elektrokhimiya, 8 (1972) 412.
37 G. Valette and A. Hamelin, J. Electroanal Chem., 45 (1973) 301.
38 T. Vitanov, A. Popov and E.S Sevastyanov, Elektrokhimiya, 12 (1976) 582.
39 T Vitanov, A. Popov, E.S. Sevastyanov, J. Electroanal. Chem , 142 (1982) 289.

40 G. Valette, J Electroanal. Chem., 122 (1981) 285.
41 E S. Sevastyanov, M.N Ter-Akopyan and V K Chubarova, Electrokhimiya, 16 (1980) 432
42 A.G. Zelinsky and R Yu Beck, Elektrokhimiya, 14 (1978) 1825
43 A. Frumkin and A. Gorodezkaja, Z. Phys Chem , 136 (1928) 451.
44 C Herring and M H. Nichols, Rev Mod Phys , 21 (1946) 185.
45 G Valette, C.R. Acad. Sci. (Paris), 273C (1971) 320
46 I.A. Bagotskaya, B.B. Damaskin and M.D Levi, J. Electroanal Chem , 115 (1980) 189
47 A. Hamelin, G Valette and R. Parsons, Extended Abstracts, Part I, 29th I.S.E. Meeting, Budapest, 1978, p 372.
48 G. Valette, J Electroanal. Chem., 138 (1982) 37
49 G. Valette, A. Hamelin and R Parsons, Z. Phys Chem N F., 113 (1978) 71.
50 A Hamelin and G. Valette, C.R. Acad Sci (Paris), 269C (1969) 1020
51 G Valette and A. Hamelin, C.R. Acad. Sci (Paris), 279C (1974) 295
52 T. Vitanov, A. Popov and E.S Sevastyanov, Elektrokhimiya, 10 (1974) 346
53 T. Vitanov and A Popov, Dokl. Akad. Nauk. S S.S.R , 226 (1976) 373.
54 T Vitanov and A Popov, Extended Abstracts, Vol. 1, 28th I S E. Meeting, Varna, 1977, p 230.
55 T. Vitanov and A. Popov, Extended Abstracts, Vol. 1, 29th I S.E. Meeting, Budapest, 1978, p 379
56 T Vitanov and A. Popov, Elektrokhimiya, 12 (1976) 319
57 G. Valette, J Electroanal. Chem., 132 (1982) 311
58 E.S. Sevastyanov, A. Shlepacov and M Kozlov, Double Layer and Adsorption on Solid Electrodes, Vol V, Tartu Univ., p. 223.
59 T. Vitanov and A Popov, Elektrokhimiya, 10 (1974) 1373.
60 M. Fleischmann, J. Robinson and R Waser, J. Electroanal. Chem , 117 (1981) 257
61 M.M. Andrusev, A.B. Ershler and G A. Tedoradze, Elektrokhimiya, 6 (1970) 1159
62 A. Tadjeddine, D M Kolb and R. Kotz, Surf. Sci., 101 (1980) 277.
63 A. Tadjeddine and D.M. Kolb, Le Vide, No. 201 (1980) 615.
64 W Boeck and D.M. Kolb, Surf Sci , accepted for publication
65 H.A. Laitinen and S.M Chao, J. Electrochem. Soc., 108 (1961) 726.
66 M Petit and J Clavilier, C.R Acad. Sci (Paris), 265C (1967) 145
67 A Hamelin, J. Electroanal. Chem., 138 (1982) 395.
68 A Hamelin, M Sotto and G Valette, C.R. Acad Sci (Paris), 268C (1969) 213.
69 A Hamelin and J Lecoeur, Collect. Czech Chem Commun , 36 (1971) 714
70 A. Hamelin and P. Dechy, C.R. Acad. Sci (Paris), 272C (1971) 1450
71 A. Hamelin and J.P. Bellier, J. Electroanal Chem., 41 (1973) 179.
72 A Hamelin and P. Dechy, C.R Acad Sci. (Paris), 276C (1973) 33.
73 A Hamelin and J.P Bellier, C R Acad Sci. (Paris), 279C (1974) 371
74 J. Lecoeur and A Hamelin, C.R. Acad. Sci. (Paris), 279C (1974) 1081
75 A Hamelin and J.P Bellier, C R Acad Sci. (Paris), 279C (1974) 481
76 J.P. Bellier and A. Hamelin, C R. Acad Sci. (Paris) 280C (1975) 1489
77 J. Lecoeur, C. Sella, J C. Martin, K Tertian and J. Deschamps, C.R Acad Sci. (Paris), 281C (1975) 71
78 J Lecoeur, C.R. Acad. Sci. (Paris), 283C (1976) 651
79 A. Hamelin and J Lecoeur, Surf Sci., 57 (1976) 771
80 A. Hamelin and J.P Bellier, Surf. Sci , 78 (1978) 159.
81 C Nguyen Van Huong, C Hinnen, J Lecoeur and R. Parsons, J. Electroanal. Chem., 92 (1978) 239.
82 J. Dalbera, J. Lecoeur and A. Rousseau, Le Vide, 4ème Coll. Phys Chim Surf , 1978, p 135
83 J Lecoeur, A. Hamelin, C. Sella and J.P. Martin, Le Vide, 4ème Coll Phys Chim. Surf., 1978, p 143
84 J P Ganon, C. Nguyen Van Huong and J. Clavilier, Surf Sci , 79 (1979) 245.
85 C. Nguyen Van Huong, C Hinnen and J. Lecoeur, J. Electroanal. Chem., 106 (1980) 185
86 A Hamelin and J P Bellier, Le Vide, 4ème Conf. Internationale sur les Surfaces Solides, 1980, p. 594.

87 C Hinnen and R Parsons, Le Vide, 4ème Conf Internationale sur les Surfaces Solides, 1980, p 630
88 C Nguyen Van Huong, C. Hinnen and R. Parsons, J. Electroanal Chem., 105 (1979) 397
89 A. Hamelin, J. Electroanal Chem , 101 (1979) 285
90 R. Kofman, R. Garrigos and P. Cheyssac, Surf. Sci , 101 (1980) 231
91 A. Hamelin, J. Clavilier, C. Nguyen Van Huong and G. Valette, Meeting on the Electrical Double Layer, Society for Electrochemistry, Bristol, 1972
92 A. Hamelin, G. Valette and J P Bellier, Extended Abstracts 25th I S E. Meeting, Brighton, 1974, p 277.
93 C. Nguyen Van Huong, C. Hinnen, J.P Dalbera and R Parsons, J Electroanal Chem., 125 (1981) 177.
94 J Lecoeur, J Andro and R. Parsons, Surf Sci., 114 (1982) 320
95 J P Bellier, J Electroanal. Chem., 140 (1982) 391
96 A Hamelin, J. Electroanal. Chem., 142 (1982) 299
97 A. Hamelin, J Electroanal Chem , 144 (1983) 365
98 J. Lipkowski, C Nguyen Van Huong, C. Hinnen, R Parsons and J. Chevalet, J. Electroanal Chem., 143 (1983) 375
99 A Hamelin and A. Lelan, C R Acad. Sci. (Paris), 295, série II (1982) 161.
100 A Hamelin and J.P. Bellier, J. Electroanal Chem., to be published
101 L Peralta, Y. Berthier and J. Oudar, Le Vide, 4ème Coll. Phys. Chim Surf. Sol., 1978, p 83
102 J Clavilier and C. Nguyen Van Huong, J Electroanal Chem , 80 (1977) 101
103 A G. Zelinsky, R.Yu. Beck, A.L. Makurin and S D. Abdulov, Elektrokhimiya, 14 (1978) 1740
104 C. Hinnen, C Nguyen Van Huong and J.P. Dalbera, J. Chim Phys , 79 (1982) 37
105 I.M. Novoselskiy, N.I. Maximuk and L.Ya. Egorov, Elektrokhimiya, 9 (1973) 1518.
106 I M Novoselskiy, N I. Konevskih and L.Ya Egorov, Double Layer and Adsorption on Solid Electrodes, Vol. III, Tartu Univ , 1972, p. 195.
107 V V. Batrakov and H. Hennig, Elektrokhimiya, 13 (1977) 259
108 N.I. Maximuk and L Ya. Egorov, Double Layer and Adsorption on Solid Electrodes, Vol IV, Tartu Univ., 1975, p 177.
109 N.I. Maximuk, Double Layer and Adsorption on Solid Electrodes, Vol. V, Tartu Univ , 1978, p 148
110 H. Hennig and V V Batrakov, Elektrokhimiya, 15 (1979) 1833.
111 G Clark, T Andersen, R. Valentine and A Eyring, J. Electrochem. Soc , 121 (1974) 618
112 V.V Batrakov, U Drittrih and A N Popov, Double Layer and Adsorption on Solid Electrodes, Vol III, Tartu Univ., 1972, p 45.
113 A.I Sidnin and V.V. Batrakov, Double Layer and Adsorption on Solid Electrodes, Vol III, Tartu Univ , 1972, p. 230.
114 A.N. Frumkin, V.V Batrakov and A.I. Sidnin, J. Electroanal. Chem , 39 (1972) 225
115 V.V Batrakov and Yu.P Ipatov, Elektrokhimiya, 11 (1975) 1287
116 V.Ya Bartenev, E S Sevastyanov and D.I Leikis, Elektrokhimiya, 6 (1970) 1197.
117 P. Caswell, N A. Hampson and D Larkin, J Electroanal. Chem , 20 (1969) 335
118 A I. Danilov, V.V. Batrakov and V A. Safonov, Elektrokhimiya, 16 (1980) 100.
119 B.B. Damaskin and V V. Batrakov, Elektrokhimiya, 10 (1974) 140.
120 I.A. Abdullin, V.A Golovin and N.V. Gudin, Double Layer and Adsorption on Solid Electrodes, Vol. II, Tartu Univ., 1970, p. 52
121 V V. Batrakov and A I. Sidnin, Elektrokhimiya, 8 (1972) 743.
122 V.V. Batrakov, A N Frumkin and A.I. Sidnin, Elektrokhimiya, 10 (1974) 216, V.V Batrakov and A I. Sidnin, Elektrokhimiya, 10 (1974) 1757.
123 V V. Batrakov and B B. Damaskin, J. Electroanal Chem., 65 (1975) 361
124 V V. Batrakov, B.B Damaskin and Yu.P. Ipatov, Elektrokhimiya, 10 (1974) 144
125 Yu P. Ipatov, V.V. Batrakov, Elektrokhimiya, 11 (1975) 1282
126 Yu.P Ipatov and V.V. Batrakov, Elektrokhimiya, 11 (1975) 1717.
127 Yu P Ipatov and V V. Batrakov, Elektrokhimiya, 12 (1976) 1174.
128 Yu P. Ipatov and V.V. Batrakov, Elektrokhimiya, 16 (1980) 624.

129 Yu P Ipatov and V V. Batrakov, Elektrokhimiya, 16 (1980) 630
130 V V Batrakov, Double Layer and Adsorption on Solid Electrodes, Vol IV, Tartu Univ , 1975, p. 33
131 L P Kmelevaya, A V. Tchijov and B B Damaskin, Elektrokhimiya, 14 (1978) 1304
132 K V Rybalka and D I Leikis, Elektrokhimiya, 3 (1967) 383
133 L P Kmelevaya, A V. Tchijov, B B. Damaskin and T.I Vainblat, Elektrokhimiya, 16 (1980) 257.
134 L.P Kmelevaya, B B Damaskin and A.I. Sidnin, Elektrokhimiya, 17 (1981) 436
135 L P Kmelevaya and B B. Damaskin, Elektrokhimiya, 17 (1981) 1721
136 L.P. Kmelevaya and B B Damaskin, Elektrokhimiya, 18 (1982) 485
137 A N. Frumkin, M P. Pyarnoya, N.B Grigoriev and U V Pal'm, Elektrokhimiya, 10 (1974) 1130
138 U V Pal'm, M.P Pyarnoya and M.A Sal've, Elektrokhimiya, 13 (1977) 873.
139 K Pal'ts, U V Pal'm, M V. Past and R. Pullerits, Uch. Zap. Tartu Univ , 235 (1969) 57
140 M P. Pyarnoya, U V Pal'm and N B Grigoriev, Elektrokhimiya, 11 (1975) 575.
141 U.V Pal'm and M P Pyarnoya, Elektrokhimiya, 16 (1980) 1599
142 Yu I Erlih and U V Pal'm, Elektrokhimiya, 10 (1974) 1866
143 Yu I Erlih, M P Pyarnoya, T.E Erlih and U V. Pal'm, Double Layer and Adsorption on Solid Electrodes, Vol. IV, Tartu Univ , 1975, p. 342
144 Yu I Erlih, T E Erlih and U V Pal'm, Elektrokhimiya, 11 (1975) 1009
145 U V Pal'm and M P. Pyarnoya, Elektrokhimiya, 14 (1978) 1070.
146 M P. Pyarnoya and U.V. Pal'm, Elektrokhimiya, 14 (1978) 1229
147 E.I Lust, M.P. Pyarnoya and U.V Pal'm, Double Layer and Adsorption on Solid Electrodes, Vol VI, Tartu Univ., 1981, p. 185
148 U V. Pal'm, M P Pyarnoya and M M. Lang, Double Layer and Adsorption on Solid Electrodes, Vol V, Tartu Univ., 1978, p 185.
149 N A Paltusova, A.R Alumaa and U V. Pal'm, Double Layer and Adsorption on Solid Electrodes, Vol. V, Tartu Univ , 1978, p. 180
150 N A Paltusova, A R. Alumaa and U.V Pal'm, Elektrokhimiya, 15 (1979) 1723
151 N A Paltusova, A R. Alumaa and U V Pal'm, Elektrokhimiya, 15 (1979) 1870.
152 N.A Paltusova, A.R. Alumaa and U V. Pal'm, Elektrokhimiya, 16 (1980) 1249
153 U V. Pal'm and M.P Pyarnoya, Elektrokhimiya, 18 (1982) 471.
154 N A Paltusova, A.R. Alumaa and U V Pal'm, Elektrokhimiya, 18 (1982) 475.
155 N A. Paltusova, A R Alumaa and U V Pal'm, Double Layer and Adsorption on Solid Electrodes, Vol VI, Tartu Univ., 1981, p. 274.
156 B B Damaskin, O A Petri and V V Batrakov, Adsorption of Organic Compounds on Electrodes, Nauka, Moscow, 1968.
157 K L Anni, Yu I Erlich and U V. Pal'm, Double Layer and Adsorption on Solid Electrodes, Vol. VI, Tartu Univ. 1981, p. 5.
158 T Vitanov, A. Popov and E S Sevastyanov, Elektrokhimiya, 11 (1975) 170